anomalies extending below 100 meter from the surface. Geology and mineralization in MJTK-1 are described as follows:

0 - 23.4 m: Pillow lava with calcite veinlets and tensional cracks filled by calcite.
23.4 - 24.2 m: Clay zone.
24.2 - 29.6 m: Hard black shale.
29.6 - 31.2 m: Black shale, sheared and argillized.
31.2 - 44.8 m: Black shale - chert breccia with shear zone. Chert fragment is dominant. (Pyrite fragments of 5 cm in maximum size are observed at 42.7 - 43.0 m.)
44.8 - 56.45m: Fine grained graywacke breccia of 10-60 cm in diameter in matrix of black shale.
56.45- 61.0 m: Clay zone with graywacke breccia.
61.0 - 64.0 m: Graywacke with bedding plane dipping 40°.
64.0 - 65.8 m: Siltstone with bedding plane dipping 60-90°.
65.8 - 78.0 m: Graywacke, black shale - chert breccia. (Fragments of pyrite aggregate at 66.7 m.)
78.0 - 85.1 m: Graywacke - siltstone breccia in matrix of black shale.
85.1 - 88.6 m: Graywacke
88.6 -105.0 m: Graywacke - siltstone breccia in matrix of black shale. Size of breccia is less than 30 cm in diameter.
105.0 -108.7 m: Black shale - siltstone.
108.7 -109.4 m: Graywacke.
109.4 -117.8 m: Graywacke breccia in matrix of black shale.
117.8 -121.5 m: Black shale - chert breccia.
121.5 -139.1 m: Graywacke breccia in matrix of black shale.
139.1 -142.0 m: Black shale.
142.0 -152.9 m: Graywacke breccia in matrix of black shale.
152.9 -154.4 m: Graywacke.
154.4 -164.25m: Graywacke breccia in matrix of black shale.
164.25-170.7 m: Black shale.
170.7 -178.65m: Graywacke intercalated by black shale.
178.65-183.25m: Graywacke breccia in matrix of black shale.
183.25-206.0 m: Black shale with bedding plane dipping 70-90°.
206.0 -241.75m: Graywacke - black shale breccia in matrix of black shale.
241.75-249.25m: Black shale.
249.25-254.6 m: Black shale breccia in matrix of clay.
254.6 -270.2 m: Graywacke breccia in matrix of black shale.
270.2 -287.85m: Black shale strongly argillized, containing a small amount of quartz and graywacke fragments.
287.85-321.45m: Massive and graded graywacke breccia in matrix of black shale.
321.45-335.4 m: Black shale containing graywacke fragments.
335.4 -340.15m: Graywacke breccia in matrix of black shale.
340.15-352.25m: Black shale - siltstone.
352.25-363.1 m: Black shale - chert breccia.
363.1 -372.5 m: Graywacke breccia in matrix of black shale. The size of breccia is less than 30 cm.
372.5 -387.7 m: Black shale chert breccia.
387.7 -401.0 m: Graywacke breccia in matrix of black shale.

MJTK-4

The drill hole MJTK-4 is located at the Station 36.5 of the Line D of CSAMT survey. It targeted to the low resistivity anomalies extending to the shallow zone from the surface. Geology and mineralization in MJTK-4 are described as follows:

0 - 2.0 m:	Graywacke, strongly weathered.
2.0 - 11.3 m:	Graywacke intercalated by black shale.
11.3 - 15.7 m:	Black shale.
15.7 - 18.6 m:	Graywacke intercalated by black shale.
18.6 - 22.8 m:	Graywacke.
22.8 - 36.3 m:	Graywacke breccia in matrix of black shale. The size of breccia is 1-20 cm.
36.3 - 45.1 m:	Black shale intercalated by graywacke breccia.
45.1 - 57.2 m:	Graywacke breccia in matrix of black shale.
57.2 - 60.4 m:	Black shale containing graywacke fragments of 1-10 cm in size.
60.4 -121.5 m:	Graywacke breccia in matrix of black shale containing pyrite lenses from 83-86 m and pyrite aggregates of 2-10 mm in diameter from 117 - 118 m in depth.
121.5 -131.0 m:	Black shale - chert breccia containing pyrite aggregates of 5-10 mm in diameter at 124 m and 130.5 m in depth.
131.0 -136.7 m:	Graywacke breccia in matrix of black shale. Pyrite lenses of 8-30 mm in size occur at 135.8 m in depth.
136.7 -151.9 m:	Black shale with bedding plane dipping 70-80°. (Pyrite dissemination is observed from 140 to 174.5 m in depth.) (Pyrite aggregates of 8-30 mm in diameter occur at 144 m, 147.4 m and 150.3 m in depth.)
151.9 -174.5 m:	Black shale - chert breccia containing numbers of pyrite aggregate and lens. The size of pyrite aggregates and lenses is 10-50 mm.
174.5 -182.4 m:	Hyaloclastite. (Pyrite veinlets from 174.4 - 177.4 m and silicification from 177.4 - 182.4 m in depth are observed.)
182.4 -192.6 m:	Black shale with bedding plane dipping 80-90°. (Pyrite lenses and films from 182.6 - 186.8 m, pyrite veinlets and dissemination from 186.8 - 189.2 m and pyrite lenses and veinlets 189.2 - 192.6 m in depth are observed.)
192.6 -200.3 m:	Hyaloclastite and massive basalt. (Silicification, pyrite dissemination and veinlets of pyrite - quartz / calcite are observed in the deeper part from 192.6 m.)

MJTK-6

The drill hole MJTK-6 is located at the Station 15.2 of the Line D of CSAMT survey. It targeted to the low resistivity anomalies extending to the shallow zone from the surface. Geology and mineralization in MJTK-6 are described as follows:

0 - 18.6 m:	Soil and talus deposits.
18.6 - 53.4 m:	Weathered massive basalt intercalated by clay zones.
53.4 - 97.5 m:	Massive basalt, partly sheared, with quartz veinlets from 83 - 84.2 m in depth.
97.5 -100.3 m:	Massive basalt, sheared and weathered with quartz - limonite veinlets.
100.3 -117.2 m:	Massive basalt with tensional cracks filled by calcite. (Pyrite dissemination is rarely observed from 116 - 117.1 m in depth.)
117.2 -123.7 m:	Black shale, sheared and argillized, containing small fragments of basalt.
123.7 -150.8 m:	Basalt, composed of hyaloclastite and massive basalt. (Hematite, quartz or calcite veinlets are observed from 137.8 - 150.8 m in depth.)

MJTK-7

The drill hole MJTK-7 is located at 30 m to southeast from the Station 14.5 of the Line F of CSAMT survey. It targeted to the low resistivity anomalies extending bellow 100 m from the surface. Geology and mineralization in MJTK-7 are described as follows:

0 - 7.1 m:	Soil and talus deposits.
7.1 - 12.4 m:	Graywacke, weathered.
12.4 - 21.3 m:	Black shale - chert - graywacke breccia in matrix of clay.
21.3 - 24.6 m:	Black shale.
24.6 - 32.3 m:	Graywacke.
32.3 - 59.5 m:	Black shale - chert breccia, containing a small amount of graywacke fragment. Pyrite aggregate of 5 mm in diameter occurs at 47.7 m in depth.
59.5 - 62.5 m:	Graywacke breccia in matrix of black shale.
62.5 - 84.8 m:	Black shale intercalated by clay zones.
84.8 -115.0 m:	Black shale - chert breccia.
115.0 -121.5 m:	Black shale.
121.5 -124.5 m:	Graywacke breccia in matrix of black shale.
124.5 -175.5 m:	Black shale - chert breccia. Pyrite lens of 3 by 15 mm occurs at 168.2 m in depth.
175.5 -190.9 m:	Graywacke breccia, composed of massive and graded ones, in matrix of black shale.
190.9 -201.7 m:	Black shale - chert breccia.
201.7 -205.0 m:	Graywacke breccia in matrix of black shale.
205.0 -211.5 m:	Siltstone - black shale. Dips of bedding plane are 70-80°.
211.5 -244.3 m:	Black shale - chert breccia, containing graywacke fragments of 0.5-15 cm in size.
244.3 -248.5 m:	Graywacke breccia in matrix of black shale.
248.5 -251.45m:	Black shale - chert breccia.

3-4-3 Mineralization

Ore minerals observed in drill cores are pyrite, marcasite, chalcopyrite, chalcocite, sphalerite, bornite and hematite. Gangue minerals are quartz, calcite and chlorite.

The occurrence of ore minerals is breccia, lens and film of sulphides in sedimentary rocks, and veinlets and dissemination of sulphides in basalt.

Ore minerals in sedimentary rocks are pyrite and marcasite. Quartz is rarely observed as gangue mineral.

Veinlets in basalt are composed of a large amount of calcite and a minor amount of copper minerals. Disseminated sulphide mostly consists of pyrite.

Drill core samples of each 2 m from 156.9 m to 200.3 m in depth of MJTK-4 where a large amount of pyrite was disseminated, were analyzed chemically. Chemical assay was made for 5 elements as Cu, S, Au, Ag and Co. Assay result is shown in Table 2-17.

Highest copper grade is 2.63% in the depth from 176.9m to 178.9m of MJTK-4. This part is composed of network and dissemination of sulfide minerals in pillow lava.

3-5 Discussion

It is interpreted from the observation of drilling cores that sedimentary rocks of the Küre Formation consist of breccia containing allochthonous blocks as graywacke, and being filled by pelitic materials. A small block of basalt occurs in pelitic rock on the surface around MJTK-4. Pelitic rocks filling breccia have schistose texture and scaly cleavages.

From the above facts, it is inferred that these sedimentary rocks constitute a mėlange. Basalt is also inferred to be a constituent of the mėlange.

Basalt of the Küre Formation is interpreted to have imbricate structures with an extension of N-S to NNW-SSE because of the surface configuration. Basalt is divided into four bodies; basalt in which the Aşıköy ore deposit occurs, basalt located at the east of the Aşıköy ore deposit, basalt in which the Bakibaba and Kızılsu ore deposits occur, basalt in which the Zemberekler mineralized zone occurs, and basalt located in eastern margin of the zone. These rocks are supposed to be located underlying the ore deposits.

Lenses and films of pyrite occurred in the shallow pelitic rocks in MJTK-4 are assumed to be of bacteria forming since pelitic rocks contain bituminous materials. Pyrite constructing veinlets and dissemination in basalt of MJTK-4 is undoubtedly considered to be hydrothermal origin. Pelitic rocks below 137m in depth have bedding planes roughly parallel to the boundary between basalt and pelitic rocks. No large tectonic separation between pelitic rocks and basalt is supposed to exist. Pelitic rock below 140m of MJTK-4 contains pyrite dissemination. The pyrite in pelitic rocks close to the boundary of both rocks is considered to be formed successively from the mineralization in the basalt.

The result of MJTK-4 located at the north-northwest of the Zemberekler mineralized zone revealed the existence of mineralized zone in this area. Some parts of this zone show

Table 2-14 Results of Microscopic Observation of Thin Sections

Drill Hole	Depth (m)	Rock Name	Mineral/Rock Fragment							Matrix						Remark
			Qz	Fd	Mm	Sh	Ct	Br	Op	Cc	Se	Ch	Bi	Cm	Bm	
MJTK-1	28.2	Black Shale	△	△					△		△	△		△	△	Schistosity
MJTK-1	87.1	Graywacke	◎	◎				△			△	△		△		
MJTK-1	132.7	Graywacke	◎	△				△	△	△	△	△		△		
MJTK-1	172.0	Graywacke	◎	◎				△		△	△	△		△		
MJTK-1	199.4	Black Shale	·	·					·	△	△	△		△	△	Schistosity
MJTK-1	228.5	Graywacke	△	△	△			△	△		△	△	△	△		Banded
MJTK-1	247.0	Shale	△	△					△		△	△		△		Schistosity
MJTK-1	323.5	Black Shale	·	·					·		△	·		△		Schistosity
MJTK-1	344.1	Black Shale	·	·					·		△	·		△		Schistosity
MJTK-1	378.0	Black Shale	·	·							△	·		△	·	Schistosity
MJTK-4	30.5	Graywacke	◎	△	△	△	△	△	·		△	△	△	△		Fd -> Se,Ch
MJTK-4	68.2	Graywacke	◎	◎			·		·	△	△	△	△	△		Fd -> Cc,Se,Ch
MJTK-4	124.2	Black Shale	△								△	△		△	△	Schistosity, Cataclastics
MJTK-4	139.7	Black Shale	△	△						△	△			△	△	Schistosity
MJTK-4	182.9	Black Shale	△	·						·	△	·		△	·	Schistosity
MJTK-4	187.5	Black Shale	△	△						△	△	△		△	△	Schistosity, Cataclastics
MJTK-7	29.6	Graywacke	△	△			△	△	△	△	△	△		△		
MJTK-7	49.0	Chert-Black Shale	·	·					·		△	·		△		Schistosity,Folding
MJTK-7	120.7	Black Shale	·	·					△		△	△		△		Schistosity
MJTK-7	148.5	Chert-Black Shale	·	·					△		△	△		△		Schistosity,Folding

Drill Hole	Depth (m)	Rock Name	Phenocryst							Groundmass						Remark
			Qz	Fd	Mm	Op				Cc	Se	Ch	Py	Mc	Qz	
MJTK-1	17.9	Altered Basalt								△	△	△			△	Ophitic
MJTK-4	181.4	Altered Basalt		◎						△	△	·	△	·		Ophitic
MJTK-4	198.0	Altered Basalt		◎						△	△	△				Porphyritic
MJTK-6	102.0	Altered Basalt								△	△	△			△	Ophitic, Cataclastic
MJTK-6	110.1	Pillow Lava								△	△				△	Ophitic
MJTK-6	130.1	Altered Basalt		◎						△	△	△			△	
MJTK-6	142.0	Altered Basalt		◎						△	△	△			△	Microspherulitic
MJTK-6	146.7	Hyaloclastite		◎						△	△				△	

Abbreviation

Qz:Quartz
Fd:Feldspar
Mm:Mafic mineral
Sh:Shale
Ct:Chert

Br:Basic rock
Op:Opaque mineral
Cc:Carbonate
Se:Sericite
Ch:Chlorite

Bi:Biotite
Cm:Clay mineral
Bm:Bituminous material
Py:Pyrite
Mc:Marcasite

◎:Abundant - Common
△:Few
·:Rare

Table 2-15 Results of Microscopic Observation of Polished Sections

Drill Hole	Depth (m)	Description	Ore Mineral							Gangue Mineral					Remark
			Py	Cp	Ct	Bo	Sp	He	Mc	Qz	Ch	Cc			
MJTK-4	135.8	Pyrite Lens	◎							△					Py:Spherical
MJTK-4	166.2	Pyrite Aggregate	△						△						Py:Spherical, Colloform
MJTK-4	181.4	Pyrite Vein/Dissemi	◎						·						
MJTK-4	182.8	Pyrite Film/Lens	△	·			·		◎						Py:Spherical, Colloform
MJTK-4	187.5	Pyrite Vein	△						△	△		◎			
MJTK-4	198.0	Pyrite Vein	△						△			◎			
MJTK-6	84.0	Cal-Py Veinlet	△						△			◎			
MJTK-6	145.0	Cal Veinlet			·	·		◎				◎			
MJTK-6	146.7	Qz Vein		·		·		·		◎	△	◎			

Abbreviation

Py:Pyrite
Cp:Chalcopyrite
Ct:Chalcocite
Bo:Bornite
Sp:Sphalerite
He:hematite
Mc:Marcasite
Qz:Quartz
Ch:Chlorite
Cc:Calcite
◎:Abundant - Common
△:Few
· :Rare

Table 2-16 Results of X-Ray Diffraction Analysis

Drill Hole	Depth (m)	Rock Name	Mineral					
			Qz	Il	Ch	Pl	Cc	Py
MJTK-1	93.0	Clay	○	△	○			
MJTK-1	126.8	Clay	○	△	○			
MJTK-1	129.7	Clay	○	△	○	・		
MJTK-1	131.0	Clay	○	△	○	・		
MJTK-1	133.4	Clay	○	△	○	・		
MJTK-1	281.5	Clay	○	△	○			・
MJTK-4	181.4	Hyaloclastite	○	・	・	△	△	△
MJTK-4	198.0	Massive Basalt	△	・	△	○	△	・
MJTK-6	121.5	Black Shale	◎	△	○	・		
MJTK-6	142.0	Massive Basalt	△		・	◎	○	△
MJTK-6	146.7	Hyaloclastite	○	△	○		○	
MJTK-7	161.0	Black Shale	◎	△	△	・		

Abbreviations

Qz:Quartz
Il:Illite
Ch:Chlorite

Pl:Plagioclase
Cc:Calcite
Py:Pyrite

◎:Abundant
○:Common
△:Few
・:Rare

Table 2-17 Assay Results of Ore Samples

No.	Hole No.	Depth(m)	Au(g/t)	Ag(g/t)	Cu(%)	S(%)	Co(%)
K301	MJTK-4	156.9 - 158.9	<0.2	1.5	0.03	0.68	<0.01
K302	MJTK-4	158.9 - 160.9	<0.2	<1.0	<0.01	0.55	<0.01
K303	MJTK-4	160.9 - 162.9	<0.2	<1.0	<0.01	0.25	<0.01
K304	MJTK-4	162.9 - 164.9	<0.2	<1.0	<0.01	0.43	<0.01
K305	MJTK-4	164.9 - 166.9	<0.2	3.9	0.01	1.12	<0.01
K306	MJTK-4	166.9 - 168.9	<0.2	1.3	<0.01	0.45	<0.01
K307	MJTK-4	168.9 - 170.9	<0.2	<1.0	0.01	0.43	<0.01
K308	MJTK-4	170.9 - 172.9	<0.2	<1.0	0.08	1.54	<0.01
K309	MJTK-4	172.9 - 174.9	<0.2	4.2	0.02	2.05	<0.01
K310	MJTK-4	174.9 - 176.9	<0.2	<1.0	0.02	4.35	<0.01
K311	MJTK-4	176.9 - 178.9	0.7	4.2	2.63	9.14	0.02
K312	MJTK-4	178.9 - 180.9	<0.2	<1.0	0.03	4.20	<0.01
K313	MJTK-4	180.9 - 182.9	1.9	1.7	0.02	7.99	<0.01
K314	MJTK-4	182.9 - 184.9	<0.2	6.7	0.20	3.30	<0.01
K315	MJTK-4	184.9 - 186.9	<0.2	1.9	0.02	3.13	<0.01
K316	MJTK-4	186.9 - 188.9	<0.2	<1.0	0.02	4.02	<0.01
K317	MJTK-4	188.9 - 190.9	<0.2	19.0	0.04	5.77	<0.01
K318	MJTK-4	190.9 - 192.9	<0.2	9.4	0.03	4.23	<0.01
K319	MJTK-4	192.9 - 194.9	<0.2	1.2	0.02	9.43	<0.01
K320	MJTK-4	194.9 - 196.9	<0.2	9.7	0.02	5.71	<0.01
K321	MJTK-4	196.9 - 198.9	<0.2	<1.0	0.02	2.95	<0.01
K322	MJTK-4	198.9 - 200.3	<0.2	4.2	0.02	2.46	<0.01

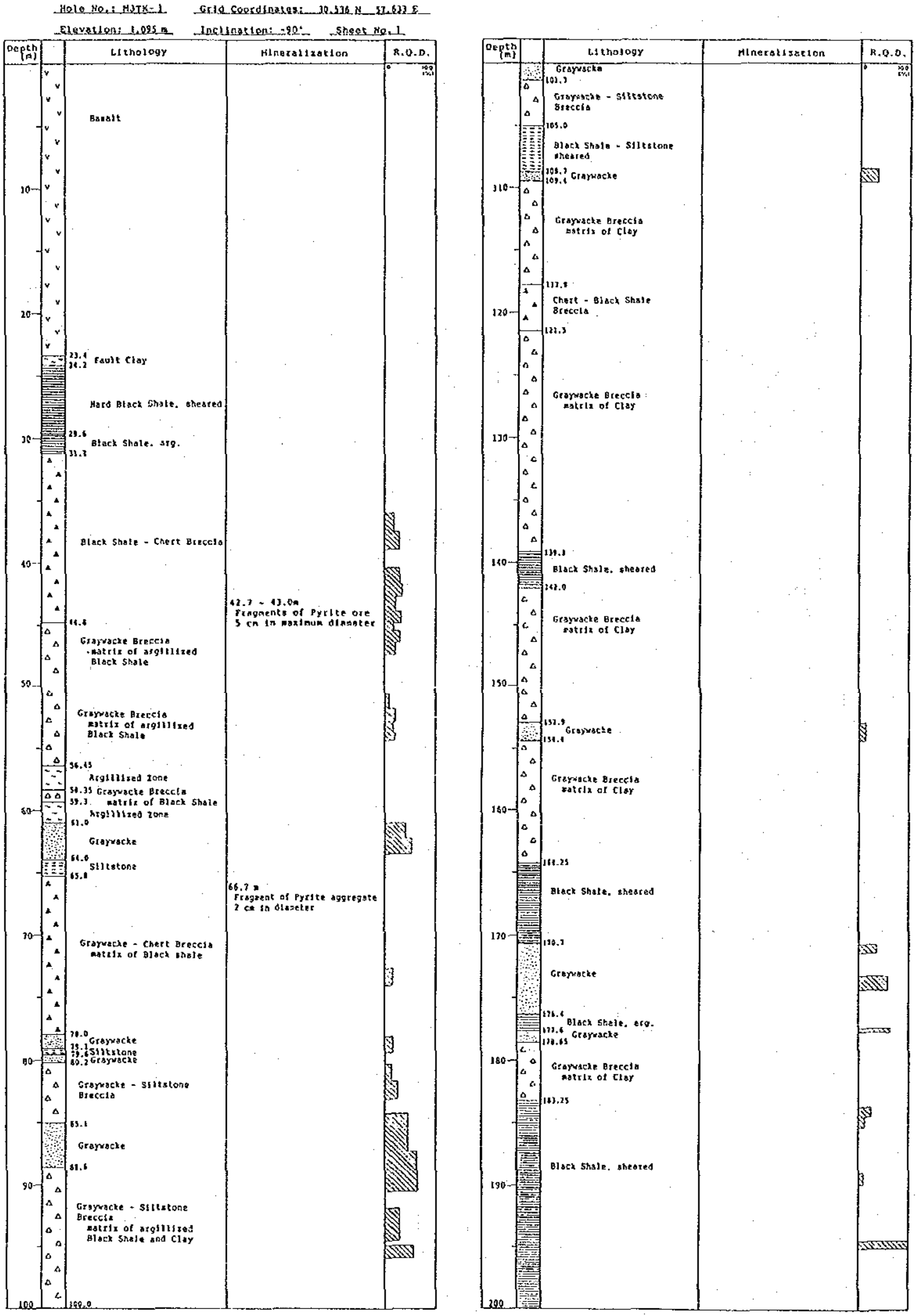

Fig. 2-10-1 Summary of Drill Logs (MJTK-1, 0-200m)

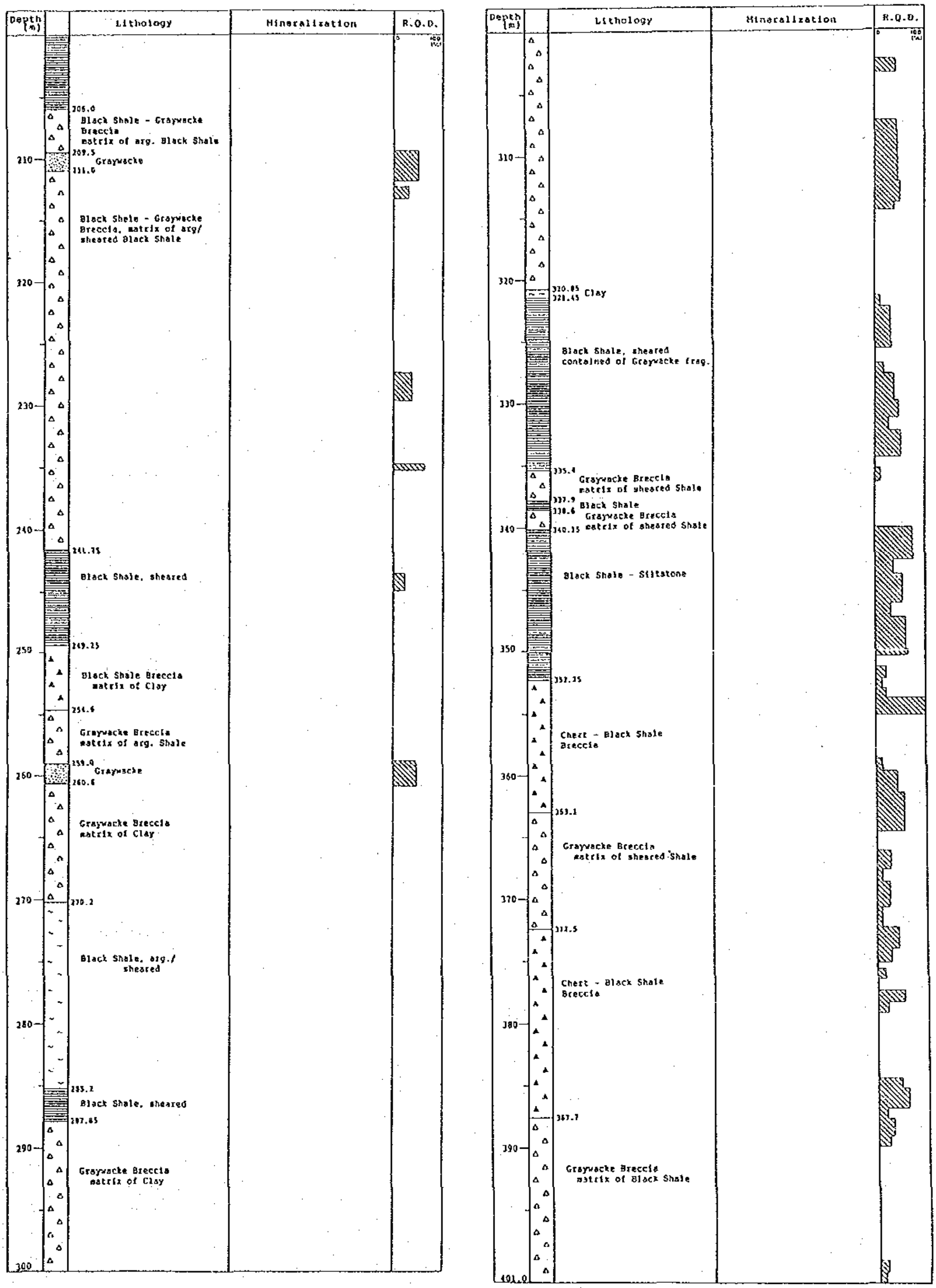

Fig. 2-10-2 Summary of Drill Logs (MJTK-1, 200-401.0m)

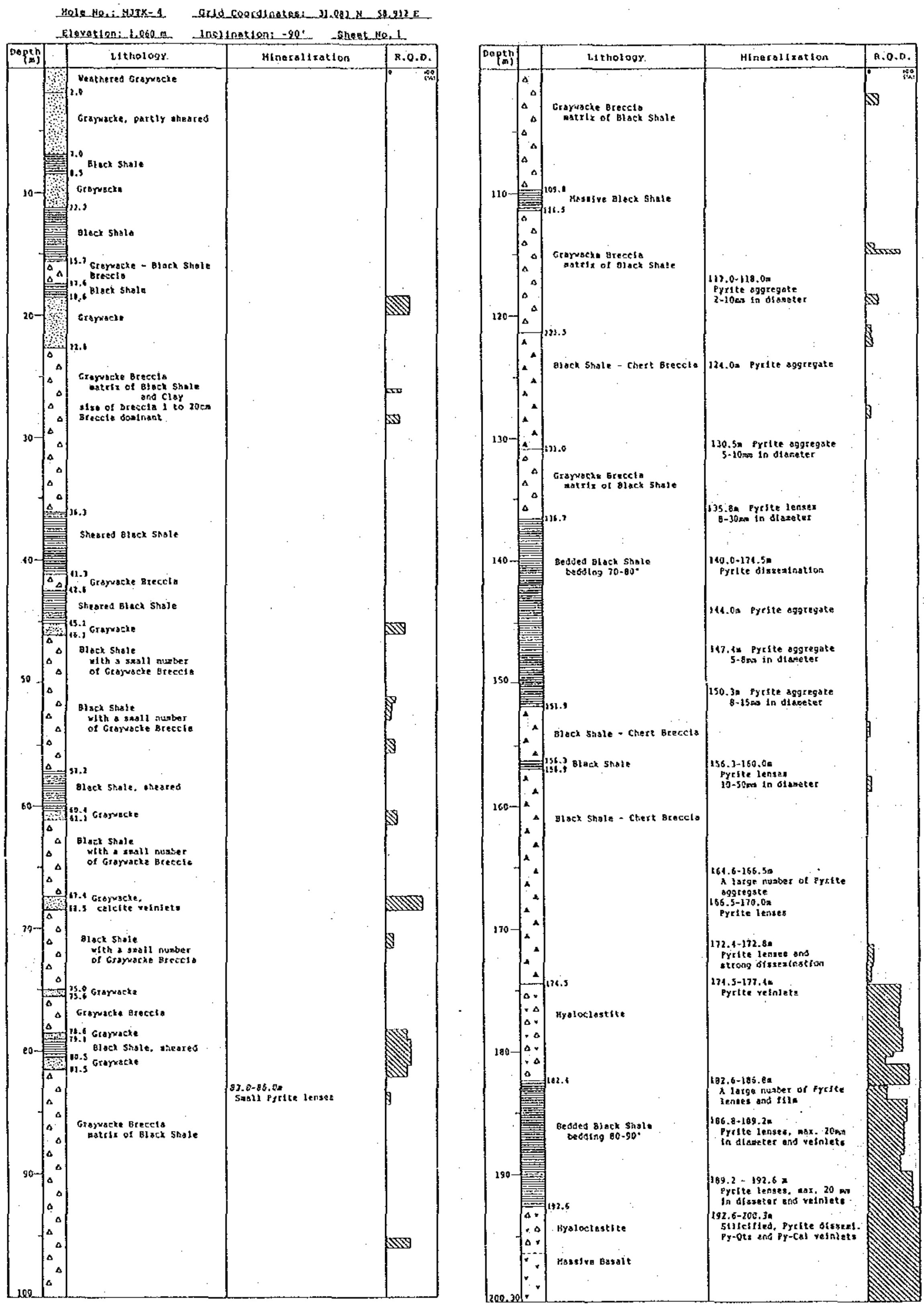

Fig. 2-11 Summary of Drill Logs (MJTK-4)

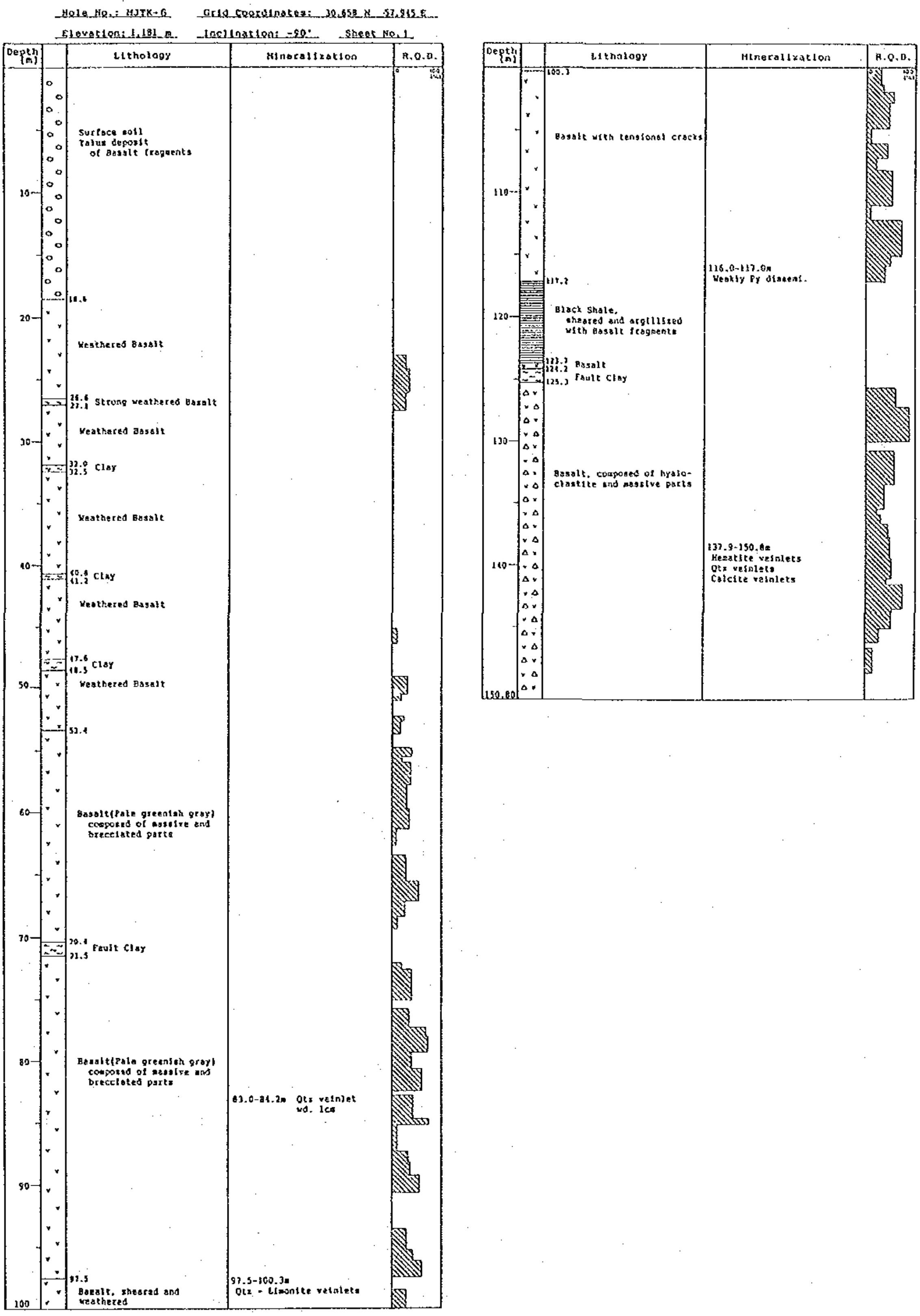

Fig. 2-12 Summary of Drill Logs (MJTK-6)

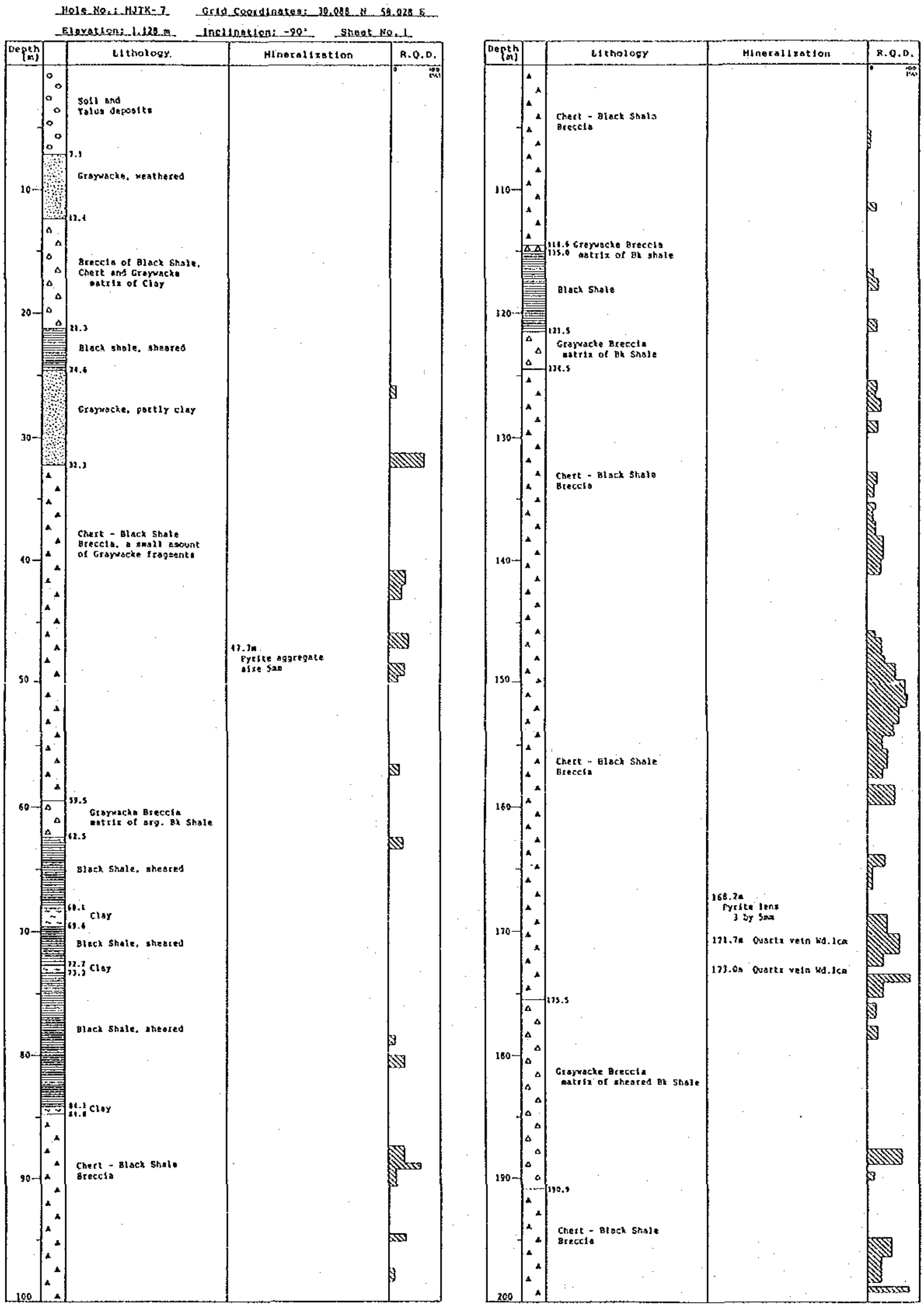

Fig. 2-13-1 Summary of Drill Logs (MJTK-7, 0-200m)

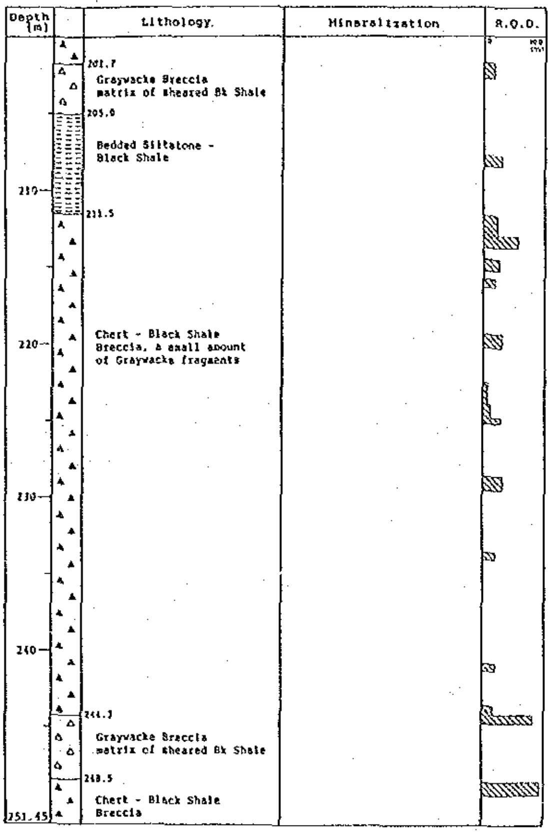

Fig. 2-13-2 Summary of Drill Logs (MJTK-7, 200-251.45m)

significant copper grades. The mineralized zone is composed of veinlets, network and dissemination of sulphide minerals in pillow lava. It is presumed that cupriferous massive ore deposit occurs adjacent to the mineralized zone. Since hyaloclastite being the host rock of the known ore deposits tends to be situated on the flank of and above pillow lava, ore deposits are possibly expected to occur between hyaloclastite and pelitic rocks.

Chapter 4 ELECTRIC LOGGING

4-1 Outline

The low CSAMT resistivity anomalies were drilled and electric logging was carried out for the drill holes in order to clarify the physical characteristics of the country rocks and the mineralized zones.

The quantity of the electric logging is follows

MJTK-4 : 200m
MJTK-6 : 120m
Total length of logging :320m

4-2 Equipment

The GEOLOGGER 3400 manufactured by OYO in Japan was used for this electric logging. The specification is as follows.

Number of channel	: two channels
Range of measuring	: 50/100/200/500/1K/2k/5k /10k/20k/50k CPS/ohm-m/F.S.
Clearance of electrode	: a=50cm, 100cm
Winding speed	: 0 - 20 m/min.
Length of cable	: 1000 m
Analog recorder	: two pens ,250m/m width, scale 1/50, 1/100, 1/200, 1/500
Power requirement	: AC 100 volts, 50/60 Hz, 30 VA

4-3 Results of Logging - MJTK-4 -

After completion of the hole at 200.3m depth, The strainers by polyvinyl chloride were immediately inserted and logging was carried out. There was a weak collapse at 120m depth, but insertion was completed after several attempts.

The following was clarified by this logging.

0 - 174.5m: Mainly black shale, resistivity 70-100ohm-m with small variation. Several resistivity peaks inferred to be caused by graywacke pebbles.
174.5 - bottom: High resistivity due to basalt.
176.9 - 178.9m: Cu 2.6% ore, but resistivity decrease

from 120 - 200ohm-m to 80ohm-m. This particularly evident with electrode interval of 50cm.
182.5 - 186.8m: Pyrite dissemination, resistivity decrease to 70ohm-m from 200ohm-m.
Bottom: Sudden increase of resistivity due to silicification of basalt.

It is seen from the above that since the ores at 176.9 - 178.9m. and the pyrite dissemination between 182.5- 186.8m are not sufficiently large to cause the CSAMT anomalies, it is reasonable to consider the source of these low resistivity to the existence of black shale to 175m depth.

4-4 Results of logging - MJTK-6 -

After completion of the hole at 150.3m depth, The strainers by polyvinyl chloride were immediately inserted and logging was carried out. There was a collapse at 120m depth, unfortunately insertion was not completed below 120m .

The following was clarified by this logging.

18.6 - 120.0m: Mainly basalt, resistivity 80-300ohm-m with comparatively wide variation. Several resistivity dips inferred to be caused by tensional cracks
105 - 120: High resistivity due to basalt.
117.2-123.7m: the resistivity are decreased by black shale .

It is seen from the above that it is reasonable to consider the source of these low resistivity to the existence of weathered basalt to 54m depth at this point.

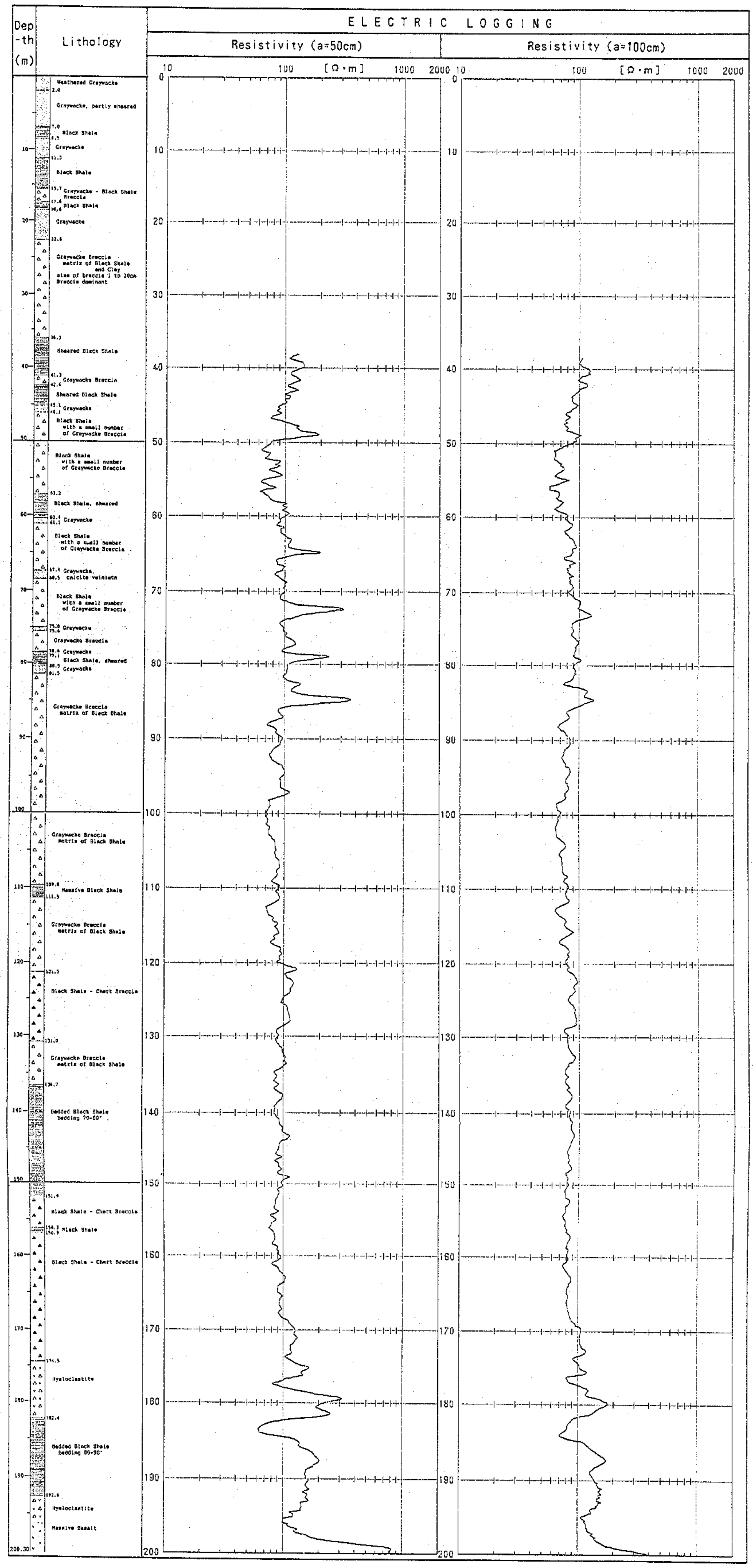

Fig. 2-14 Results of Resistivity Logging of MJTK-4

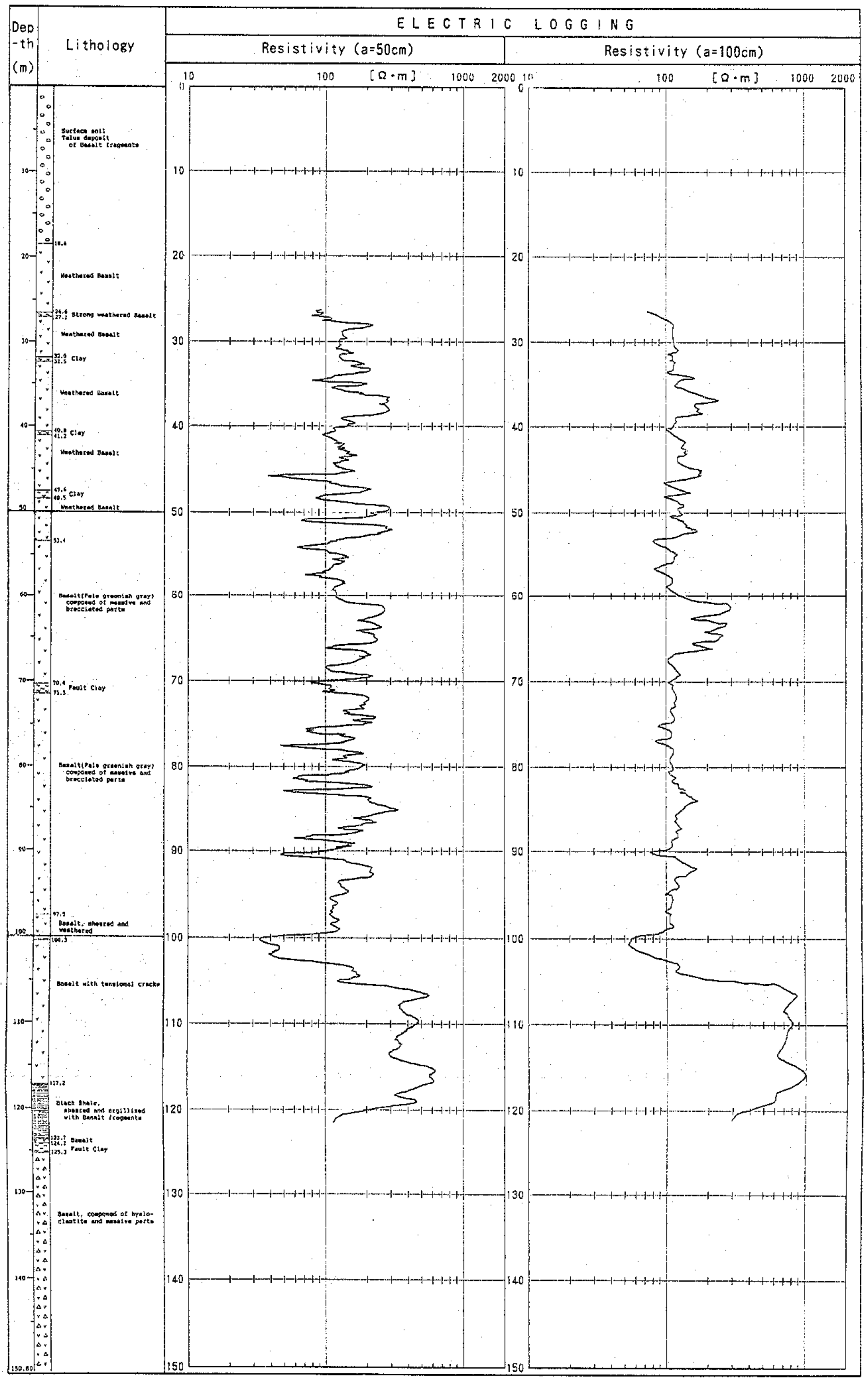

Fig. 2-15 Results of Resistivity Logging of MJTK-6

PART 3 TAŞKÖPRÜ ZONE

PART 3 TAŞKÖPRÜ ZONE

CHAPTER 1 OUTLINE OF TAŞKÖPRÜ ZONE

1-1 Outline of the Zone

The Taşköprü zone is located in the eastern part of the Küre area. This zone is situated in the northern reaches of the Gökırmak river. The western part of the zone is occupied by gently-sloping mountains with relatively low altitudes. Whereas the eastern part shows steep topography.

The main roads from Devrekani in the west of the zone and from Taşköprü in the south of the zone are passing through the north and east of the Cünür prospect. The prospect is accessible on through from these roads.
Unpaved roads reach to the center of the Cozoğlu prospect, Cozoğlu village.

Geological survey was conducted in the first phase. The Cünür and Cozoğlu prospects were extracted as the next exploration targets.
Geophysical time-domain IP survey was carried out for clarifying the geophysical properties in the deeper parts and for assessing the potential of blind deposits in the Cünür and Cozoğlu prospects.

1-2 Geology and Mineralization

(1) Cünür Prospect

The geology around the prospect is the Çangal meta-ophiolite comprising pelitic schist, massive basalt, and green schist.

Eight lenses and bedded gossans occur in green schist in the Cünür prospect. The gossans extend in the NE-SW direction which is harmonious to the bedding plane. The maximum lateral distribution is 400x50 m. The mineralization is quartz-limonite-pyrite network and limonite dissemination in the silicified and argillized parts of mafic rocks. Azurite and chrysocolla occur in some part of the gossans in the central part of the prospect. An assay result of samples is Cu 4.3 % and Zn 1.4 %. Pyrite veinlets occur in gossans in the northeastern part of the prospect with an assay result of Au 1.9 g/t, Ag 115 g/t and S 40 %. These zones are considered to be promising for copper and zinc ores. Bedded cupriferous pyrite deposits are expected below the surface, because gossans are harmoniously distributed with pelitic rocks.

(2) Cozoğlu Prospect

The geology around this prospect is composed mainly of the Çangal meta-ophiolite, the Kızacık Formation, and the Alaçam

Formation. The meta-ophiolite consists of pelitic schist, massive metabasalt and green schist. The Kızacık Formation consists of grayish white limestone. The Alaçam Formation consists of quartz arenite and black mudstone.

There are two openings of old adits on the surface. A large amount of mine wastes is found in the vicinity of openings. They are all within the Çangal meta-ophiolite.

One of the two old adits has a cross cut at 7 m from the entrance and pyrite dissemination is observed in parts of green schist with some oxidized copper minerals. Assays of these samples indicate Cu 0.7 - 0.9 % and S 1.8 %.

Another opening is supposed to be a collapsed incline or a shaft. Near the opening, there is a quartz vein of 30 cm thick in green schist with malachite flecks filled in cracks. The quartz vein shows Cu 2.5 %, Zn 0.7 %. It contains zinc oxide minerals. There are, however, many segregation quartz veins in green schist near the mineralized zone, and it is inferred that there is no relationship between the quartz vein near the adit opening and the copper oxide. A part of green schist in the vicinity is altered into gray clay.

Pyrite dissemination along the schistosity of green schist occurs in this prospect.

There are slags within 400x150 m range. Samples from two of these slags show Cu 1.0 to 4.8 %. Chalcopyrite and bornite are observed microscopically in such samples.

It is difficult to determine the type of mineralization from the surface showings. Bedded cupriferous pyrite deposit is a possible type of deposit. The reasons are; lack of strong alteration of green schist on the surface, the occurrence of copper and zinc oxide minerals, and the existence of a large amount of slags.

CHAPTER 2 GEOPHYSICAL PROSPECTING

2-1 Objective and the Outline of the Survey

Electric survey (Time-domain IP method) was applied in the Cünür and Cozoğlu areas (shown in Fig.3-1) which were considered to be promising by the geological survey carried out during 1992. The objective of the survey is to clarify the electric characteristics of the deeper subsurface zones and thus obtain information regarding the mineral potential of these zones.

The outline of the work carried out is as follows.

Cünür area

Total length of survey line	:	13,500 m
Number of survey lines	:	nine lines
Interval of lines	:	150m 300m
Points of measurement	:	414 points

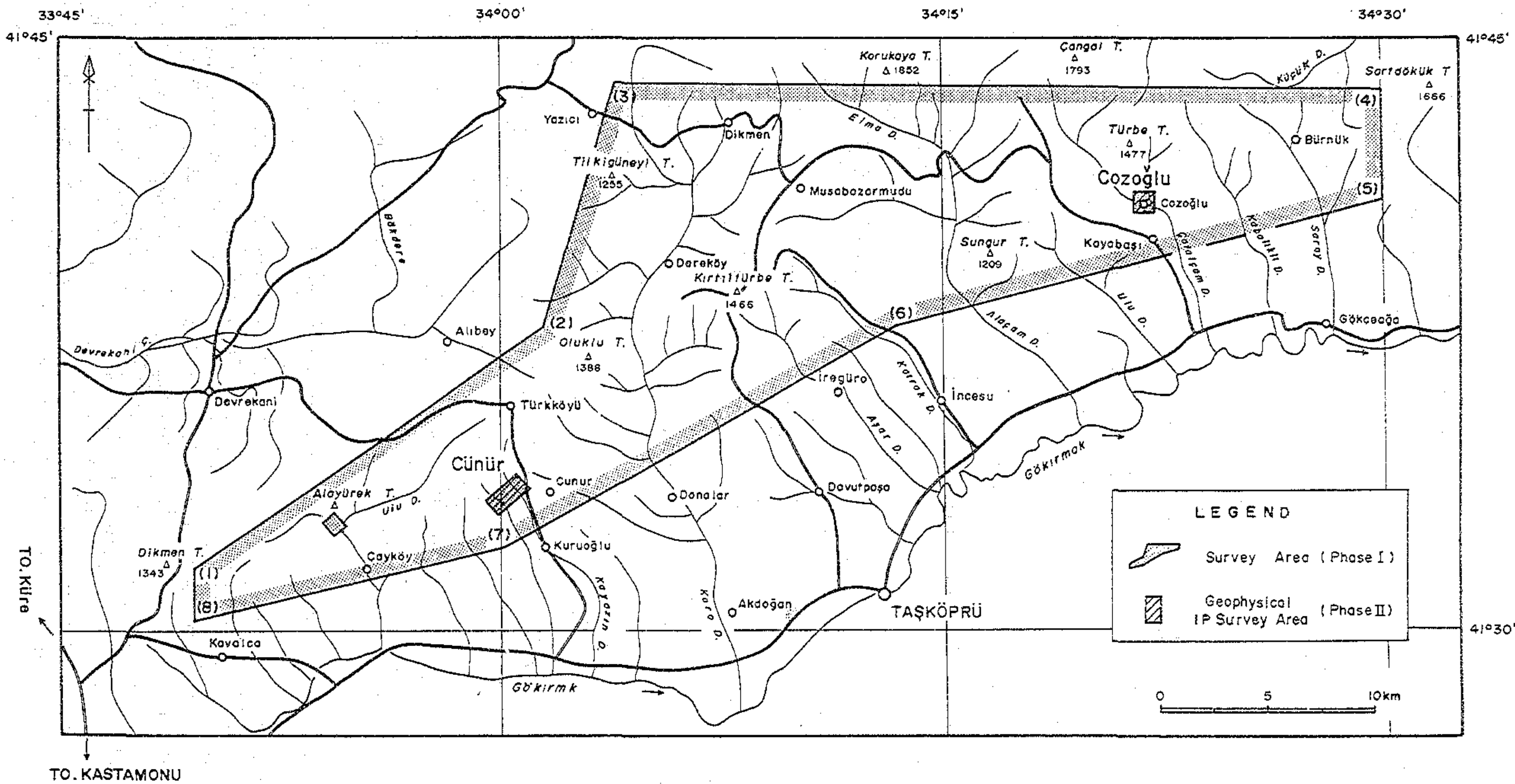

Fig. 3-1 Location Map of IP Surveys in the Taşköprü Zone

Line	Length(m)	Points of measurement
A	1,500	64
B	1,500	64
C	1,500	64
D	1,500	64
E	1,500	64
F	1,500	64
G	1,500	64
H	1,500	64
I	1,500	64

Cozoğlu area

Total length of survey line : 7,500 m
Number of survey lines : five lines
Interval of lines : 200m
Points of measurement : 230 points

Line	Length(m)	Points of measurement
A	1,500	64
B	1,500	64
C	1,500	64
D	1,500	64
E	1,500	64

Profile lines and leveling

The line intervals were set relatively wide in order to cover the total survey area with limited profile length. Interval of 300m was used for most of the Cünür area with denser profile of 150m interval in the promising zones with mineral showings. In the Cozoğlu area, 200m intervals were used.

Open traverse leveling was done by pocket compass and esron tapes.

2-2 Electric survey (Time-Domain IP method)

The electrical conduction in most rocks is essentially electrolytic, by transport of ions through interstitial water in pores. However,when a current is passed through a rock containing metallic minerals, the ionic conduction is hindered to a considerable extent by the mineral grains in which the current flow is electronic. The leads to an accumulation of ions at the interface between the minerals and solution,resulting in a growth of electrochemical voltage at the metallic grain surface. The process is similar to electrode polarization that occurs at the surface of metal electrodes dipped in an electrolyte. When the externally applied current is switched off,the electrochemical voltage is dissipated,but does not drop to zero instantaneously. The decay in voltage is observed to vary with time as shown in figure 3-2 and can be measured as a fraction of the voltage V that existed when the current was flowing. The ratio Vt/Vo gives a measure of the concentration of metallic minerals in the rock formation. This is,in brief,the principle of the induced polarization or IP method.

Induced polarization effects are observed even when metallic minerals are not present in a rock material. In particular clay-bearing sediments show an appreciable IP. The surface of a clay particle has a net negative charge which attracts positive ions from the electrolyte present in pores. As a result of this polarized distribution of ions(called the membrane polarization),current flow is impeded. When the applied current is switched off the positive ions redistribute themselves to return to an equilibrium position. This process of redistribution of ions shows a decaying voltage as an IP effect. As yet only very limited application has been made of the IP effect associated with clay minerals.

Electrode polarization, as well as the membrane polarization,is essentially a surface phenomenon. The IP effects therefore greater if the metallic ore (or clay)is disseminated rather than compact.

Time-Domain IP : Induced polarization measurements can be made either using direct current or an alternating current.

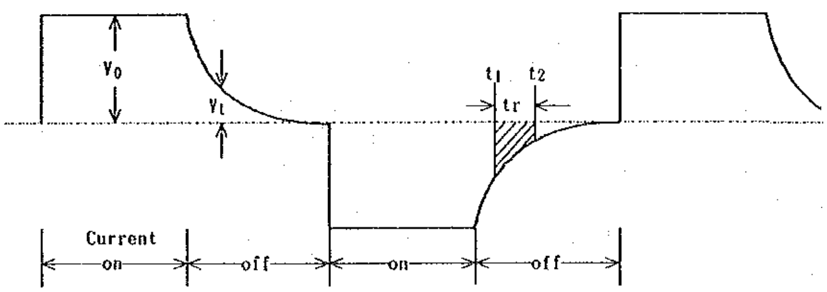

Fig. 3-2 Received Wave Form of the Time-Domain IP

When measurements are made by sending dc pulses(e.g.,of 10s duration)into the ground, the magnitude of IP is expressed as Vt/Vo where Vt is the voltage remaining at a time t ,say 2s, after the switch-off,and Vo is the voltage that existed when the current was flowing. the ratio Vt/Vo is expressed as millivolts/volt, or as a percent

$$IP\ \% = 100\ (Vt/Vo) \qquad \text{in mV/V or } \%$$

Commercial IP outfits generally register the decaying V(t) over a definite time interval(t1,t2). The result is expressed by the time-integral measure of IP as " M ".

The quantity M, known as chargeability, is commonly used in time-domain measurements of IP.

The chargeability of Scintrex IPR-12 is defined in the following calculations :

$$M = \frac{V_s * 1,000}{V_0} \qquad (mV/V)$$

Where

$$V_s = \frac{1}{t_r}\int_{t_1}^{t_2} V_t \, dt$$

t1:time at beginning of the slice
t2:time at end of slice
tr:t2-t1 (integrating period)
Vo:voltage during the current On time
Vs:voltage measured by the receiver during the integrating period with the current off.

The apparent resistivity(AR) is defined as :

AR = pai*an(n+1)(n+2) Vo/I in ohm-m

Where
a : interval of the respective dipole
n : coefficient of dipole - dipole
Vo : primary voltage of the respective dipole
I : transmitter current

2-2-1 Method of measurement

The method of IP measurement in the field is as follows: the fine receiving dipoles and transmitting dipole are set on the survey line as shown in Fig.3-3.

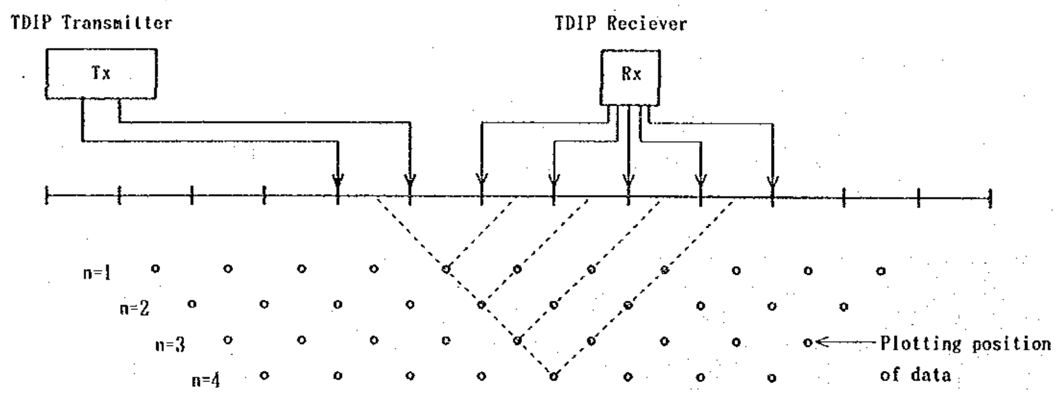

Fig.3-3 Illustration of Field Work of IP Survey

The specification of IP survey is as follows.
The configuration of electrode array : dipole-dipole
The separation of electrode : 100m
The coefficient of electrode separation : n=1 - 4
The duty cycle of on/off time : 2 sec.

2-2-2 The equipment for IP survey

The following equipments are used in this survey.

a) Receiver Scintrex IPR-12
8 channels, current on/off time 1,2,4,8,16,32 sec.
Automatic cancellation of self potential.
Preset 14 windows and automatic measuring and data storage in the semiconductor memory data.

b) Electrode of receiving dipole : porous pot with Cu-CuSO4

c) Transmitter Scintrex TSQ-3
Output power 3000AV, output voltage 300-1350 volts, output current 10 amp.
Power requirement 230volts, 3 phase, 800 Hz

d) Generator Briggs and Stratton.
Output power 3500 VA, output voltage 230 volts, 3 phase, 800Hz.

e) Electrode of transmitting dipole
stainless rods(length 50cm)

2-2-3 Analysis

The measured resistivity and chargeability values are shown in tables for each line on the profiles. The subsurface depths are shown on plane maps by the electrode separation index. And the subsurface electric characteristics can be understood from these plane maps and profiles.

The resistivity values were affected by the topography and thus terrain correction was made by using carbon paper.

Two-dimensional model simulation was carried out for IP anomalies and chargeability and resistivity values were obtained quantitatively for the anomaly sources.

2-3 Results of Analysis - Cünür Area

The location of IP survey lines in the Cünür area is shown in Fig.3-4, and geology and location of rock specimen for the laboratory test are shown in same figure.

2-3-1 Measured values

The measured apparent resistivity values are laid out for each line in Figure 3-5. These values are shown on plane maps for each depth by electrode separation index(Fig.3-6-1 to Fig.3-6-4).

The characteristics of the apparent resistivity values of this area are as follows.

a) The resistivity values are predominantly in the 100-300 ohm-m range.
b) High apparent resistivity values (>300ohm-m) are detected in the eastern part of the survey area for the shallow subsurface zones and in the northern and northwestern parts for the medium to deep zones.
c) Low apparent resistivity (<100ohm-m) is detected in the west-southwest and the central parts of the survey area for the shallow zones, and for the medium to deep zones low anomalies of small scale occur scattered throughout the survey area.

The measured chargeability values are shown for each line in Figure 3-7. These values are shown on plane maps for each depth by electrode separation index (Fig.3-8-1 to Fig.3-8-4).

The characteristics of these values are as follows

a) The chargeability values are predominantly low (<10mV/V).
b) Weak chargeability anomalies within the range of 10-50mV/V are detected for the shallow subsurface zones along Lines H - I, particularly H. For the deep zones weak anomalies are detected in the southwestern part on Line G.
c) Regarding the mineralized alteration zone at Station No. 9 on Line H where Cu 4.3% and Zn 1.4% values were obtained during the previous year, the anomaly value is only slightly higher than the vicinity and thus the mineralization is considered to be of very small scale.

Physical properties of rock samples

Resistivity and chargeability were measured for 11 samples collected from the surface in the laboratory with the field equipment under field conditions.

Table 3-1 Results of Rock Sample Measurement (Cünür Prospect)

R o c k	No.	Chargeability	Resistivity	Remarks
Massive basalt	1	1.49(mv/v)	2,122	
Silicified rock	2	1.20	1,562	
Pelitic schist	3	1.78	584	
Silicified rock	4	3.56	2,426	
Green schist	5	2.14	6,883	
Massive basalt	6	2.72	1,925	
Massive basalt	7	7.44	2,276	Pyrite Dissemi.
Massive basalt	8	3.53	2,609	
Massive basalt	9	2.56	10,095	
Massive basalt	10	1.20	540	
Silicified rock	11	5.39	4,803	Pyrite Dissemi.
Green schist	12	6.24	574	Malachite Stain

The results are as follows.

a) Many of the samples showed high resistivity exceeding 1000ohm-m and three samples showed low values near 500 ohm-m.
b) Chargeability is highest, 7.44mV/V, for massive basalt (Sample No.7) with pyrite dissemination, other samples have low values (<3.5mV) and the average of nine samples is 2.24mV/V. Samples Nos. 11 and 12 which were mineralized are exceptions. The value for No. 12 which was collected from the alteration zone is 6.24mV/V and is somewhat higher than others.

2-3-2 Results of Model Simulation Analysis

High chargeability anomalies exceeding 30mV/V in the south-eastern parts of Lines E and H and thus model simulation was carried out for these two lines as follows.

Line E (Fig.3-10-1):
The high chargeability below Stations Nos.1-5 and the high resistivity below Nos. 11-13 are the characteristics of this line. The high chargeability anomaly of Nos. 1-5 is also detected in the adjacent lines and is the most promising anomaly of this area.

In the model constructed, a high chargeability zone (15-30 mV/V) is set below Nos. 0-2, and a high resistivity anomaly on the northwestern side of this zone. Also as resistivity and chargeability increase toward the northwestern edge of this line, 15mV/V, 400ohm-m zone was established in the model at this edge.

The results of the simulation are harmonious with the measured results and thus it is considered to be a reasonable model.

The source of the anomaly in the southeastern part of this line is assumed to lie in the zone between shallow subsurface to 200m in depth. But since the total anomaly cannot be clarified by that detected at the southeastern edge of the line, it is difficult to determine whether the anomaly source is limited to the shallow parts or not.
The high resistivity in the northwestern part corresponds to the distribution of meta-basalt and green schist bodies and mineralization in the deeper zones is anticipated.

Line H (Fig.3-10-2):
In this line, 30mV/V anomaly was detected at Nos. 1-3 and negative chargeability in the deeper zone under Nos. 4-6. Also gossan containing azurite and chrysocolla occurs near No. 9. The resistivity of the most part in within the range of 150-250ohm-m and somewhat high zones over 200ohm-m occur in the central part and at the northwestern edge of the line.

In the model, 40mV/V, 150-300ohm-m zone was established at the southeastern edge of the line and a zone with higher chargeability(15mV/V) than the background in the shallow part below Nos.3-7.

Figures and contours harmonious with the measured values were obtained by the simulation. The high chargeability and resistivity at the southeastern end of this line is interpreted to indicate the possible occurrence of sulfide minerals accompanied by silicification.

2-3-3 Discussions

The results of careful analysis and interpretation of the model simulation results and the tests on the collected rock samples indicate the following.

Time-domain IP survey was carried out in an area centered around the silicified zone discovered by the geological survey of the previous year. Anomalies related to the outcrops of gossan and other evidences of mineralization confirmed on the surface could not be detected. Although the silicified zone is distributed widely in the survey area, high resistivity do not occur in this zone, while such anomalies exceeding 300ohm-m occur in the unaltered northwestern and eastern parts of the area. This indicates that the silicification is not strong and the existence of mineralization comprising magnetite, pyrrhotite and other sulfide minerals lowered the resistivity.

The chargeability values are generally not high in this area, they range in the order of 5-10mV/V (background). This is interpreted to be the result of relatively weak mineralization or oxidation or leaching of the sulfide minerals which accompanied silicification. The electrode interval of this survey was relatively large at 100m and it is difficult to detect small deposits and narrow mineralized zones. Information is available only to the depth of 250m and if oxidation and leaching occur to this depth, the low chargeability of the silicified zone can be explained.

Two profile lines were added for studying the weak anomaly (>20mV/V, Lines D and E) detected in the southeastern part of the survey area and the promising gossan discovered in the previous year.

The weak anomaly is continuous in the E-W direction which is the same as the trend of the elongation of the known gossan and it has the shape of anomalies of the dissemination deposits. This weak anomaly extends westward and wedges out at Line F in the shallow zones, but is considered to continue to the weak anomaly of Nos. 5-7 of Line F. This is considered to be caused by sulfide dissemination because of the relatively high resistivity at 150ohm-m, chargeability of 20-30mV/V and the relatively wide spread of the anomaly. The chargeability plane of -200m and -250m indicate that this anomaly connects with that of Line G and is elongated in the E-W to NE-SW direction as one mineralized zone.

Regarding the mineralized alteration zone of Lines E and

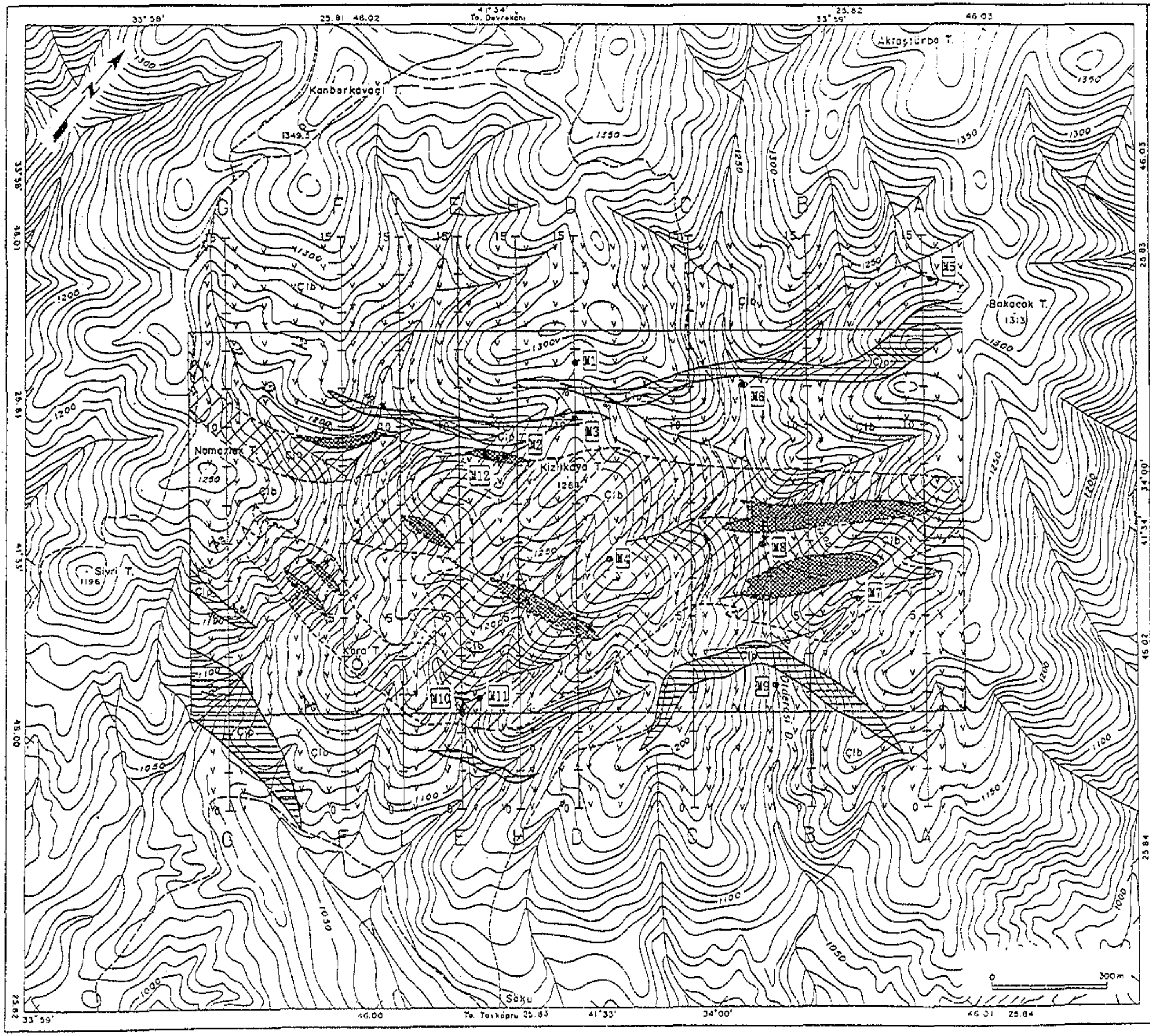

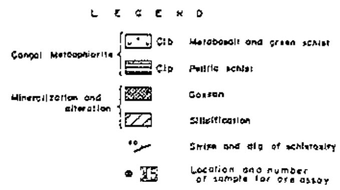

Fig. 3-4
Location Map
of IP Survey Lines
in the Cünür Prospect

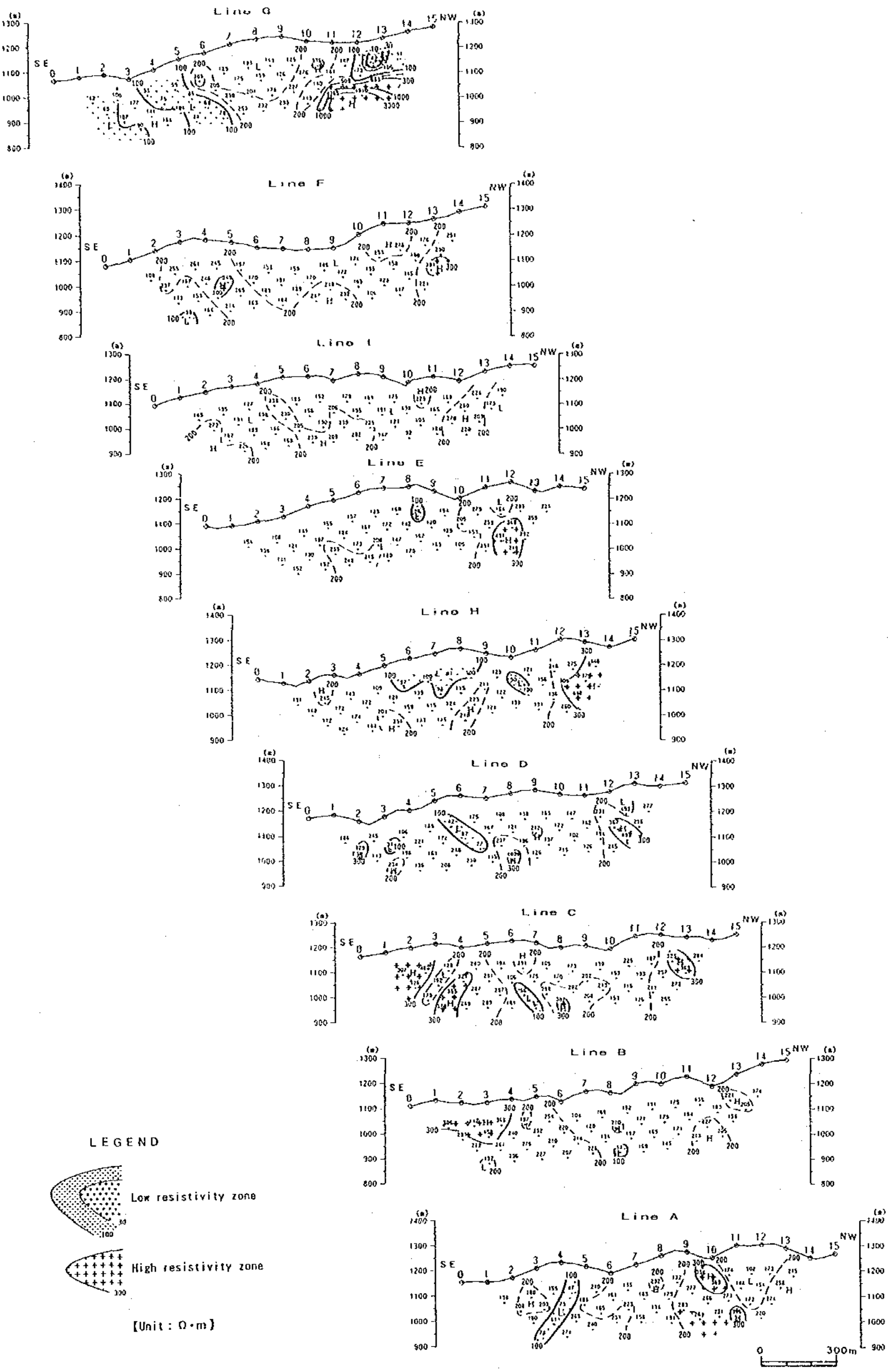

Fig. 3-5 Sections of Apparent Resistivity (Line A ～ I)

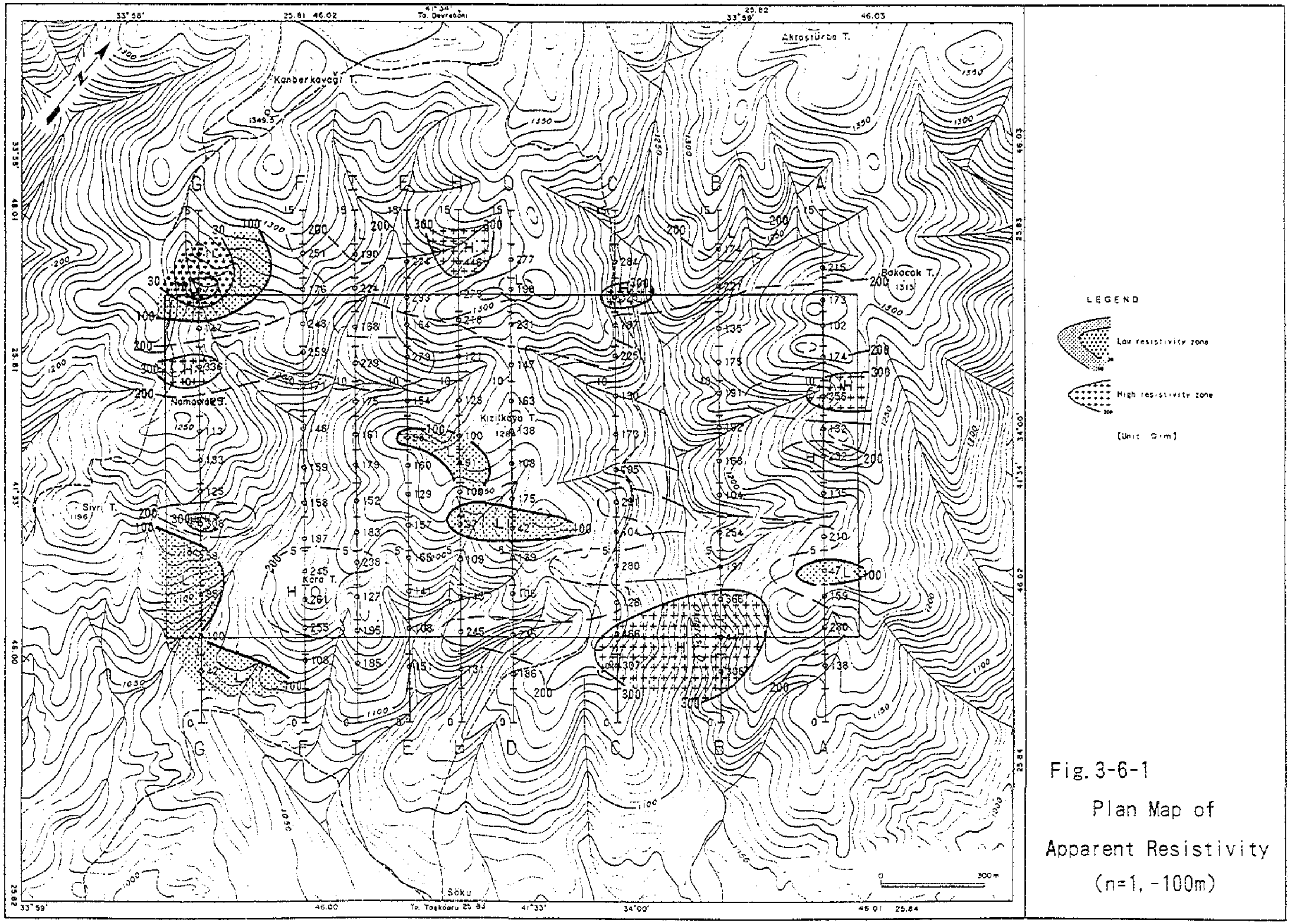

Fig. 3-6-1
Plan Map of
Apparent Resistivity
(n=1, -100m)

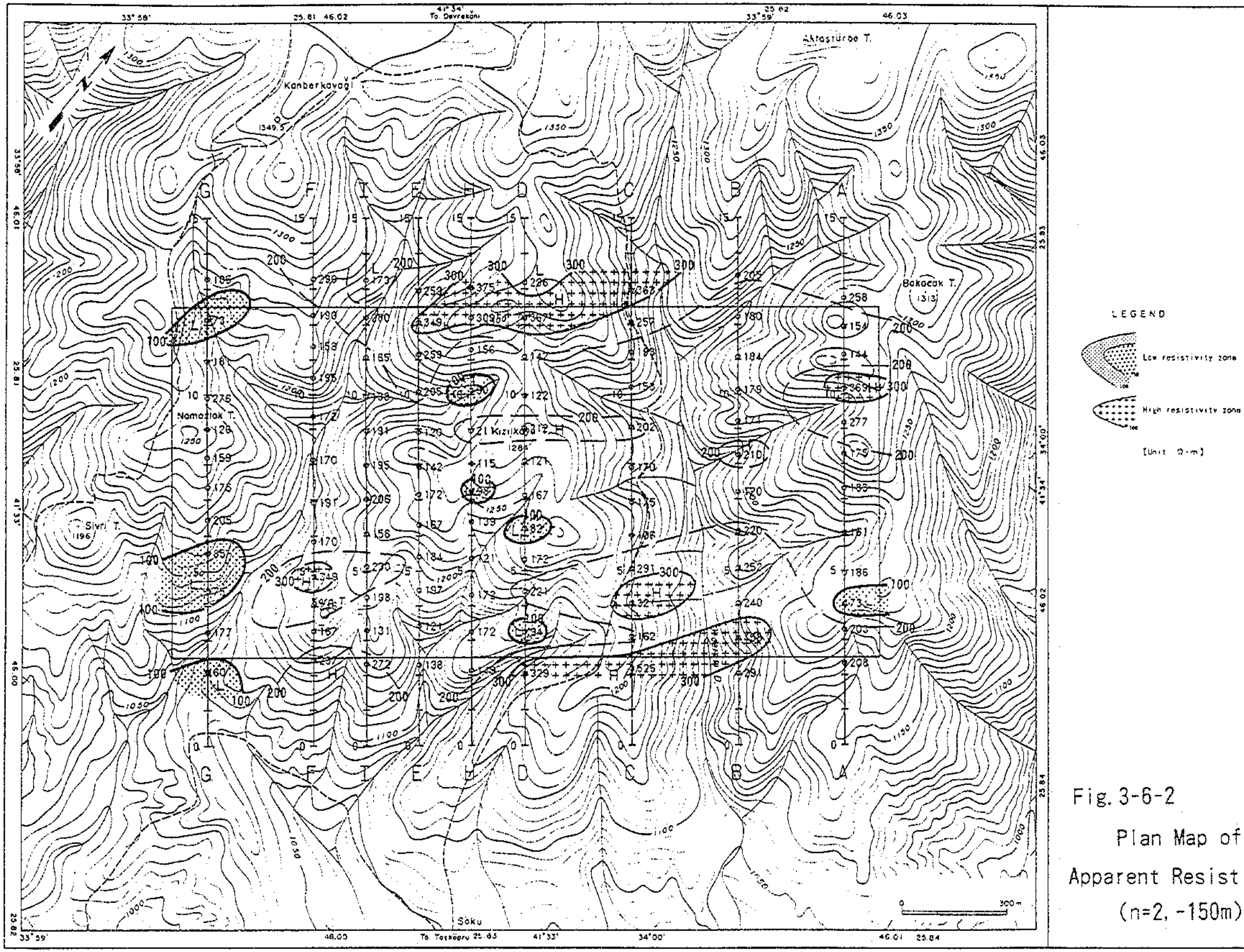

Fig. 3-6-2
Plan Map of
Apparent Resistivity
(n=2, -150m)

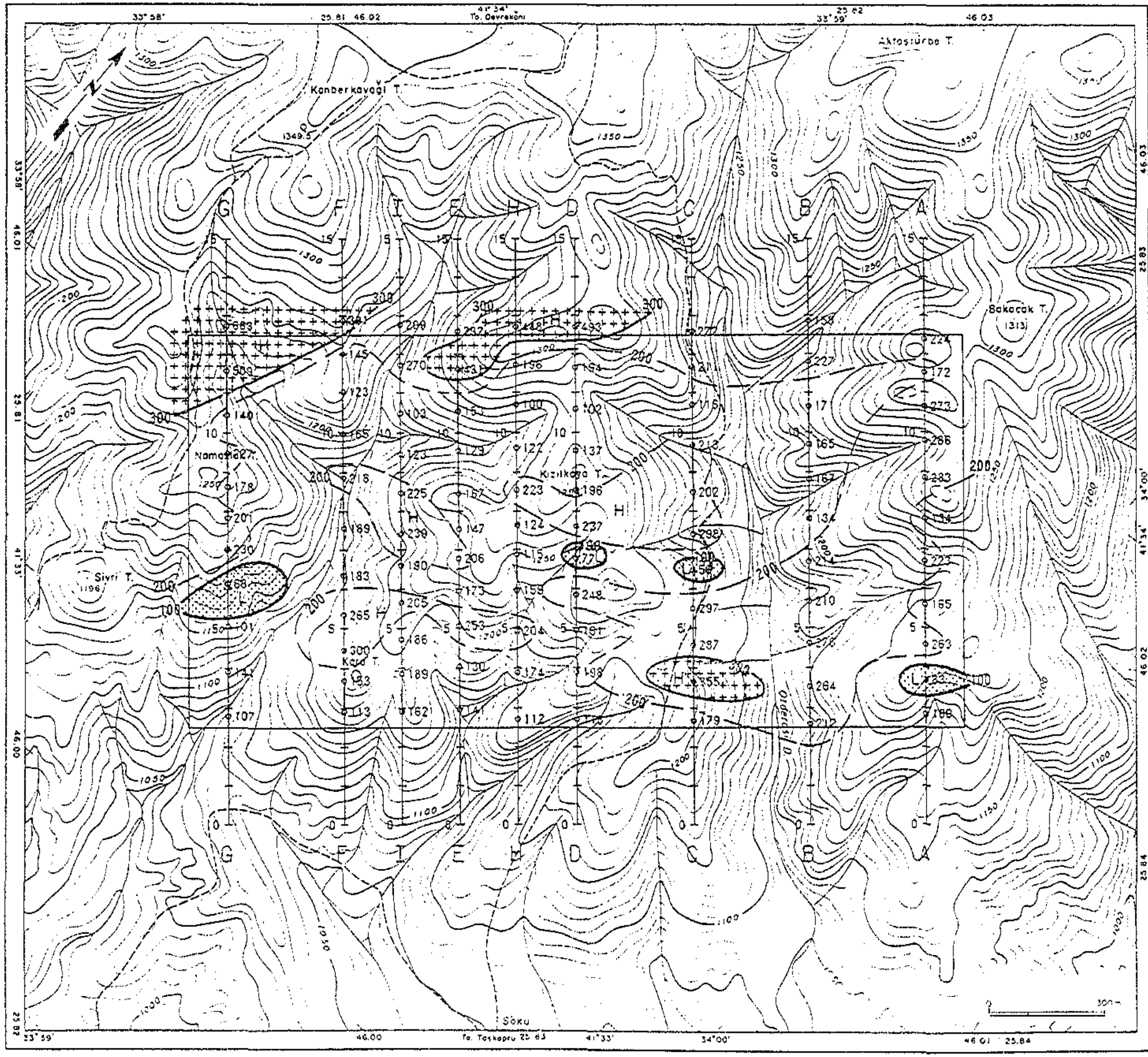

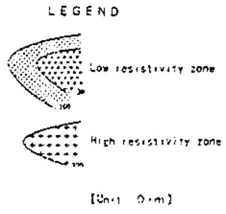

Fig. 3-6-3
Plan Map of
Apparent Resistivity
(n=3, -200m)

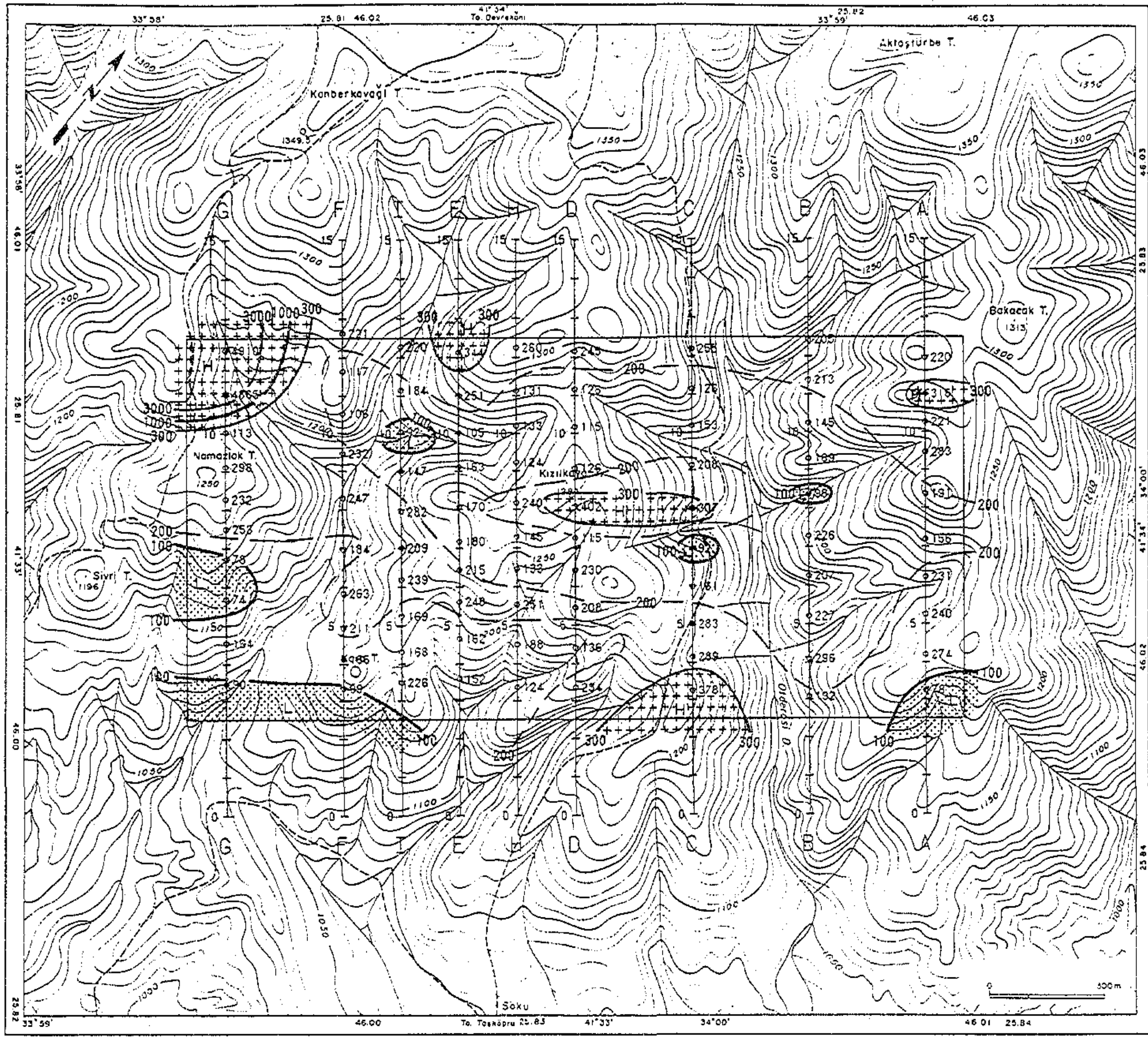

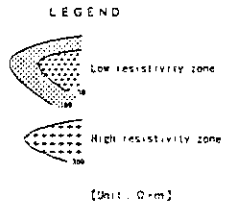

Fig. 3-6-4
Plan Map of
Apparent Resistivity
(n=4, -250m)

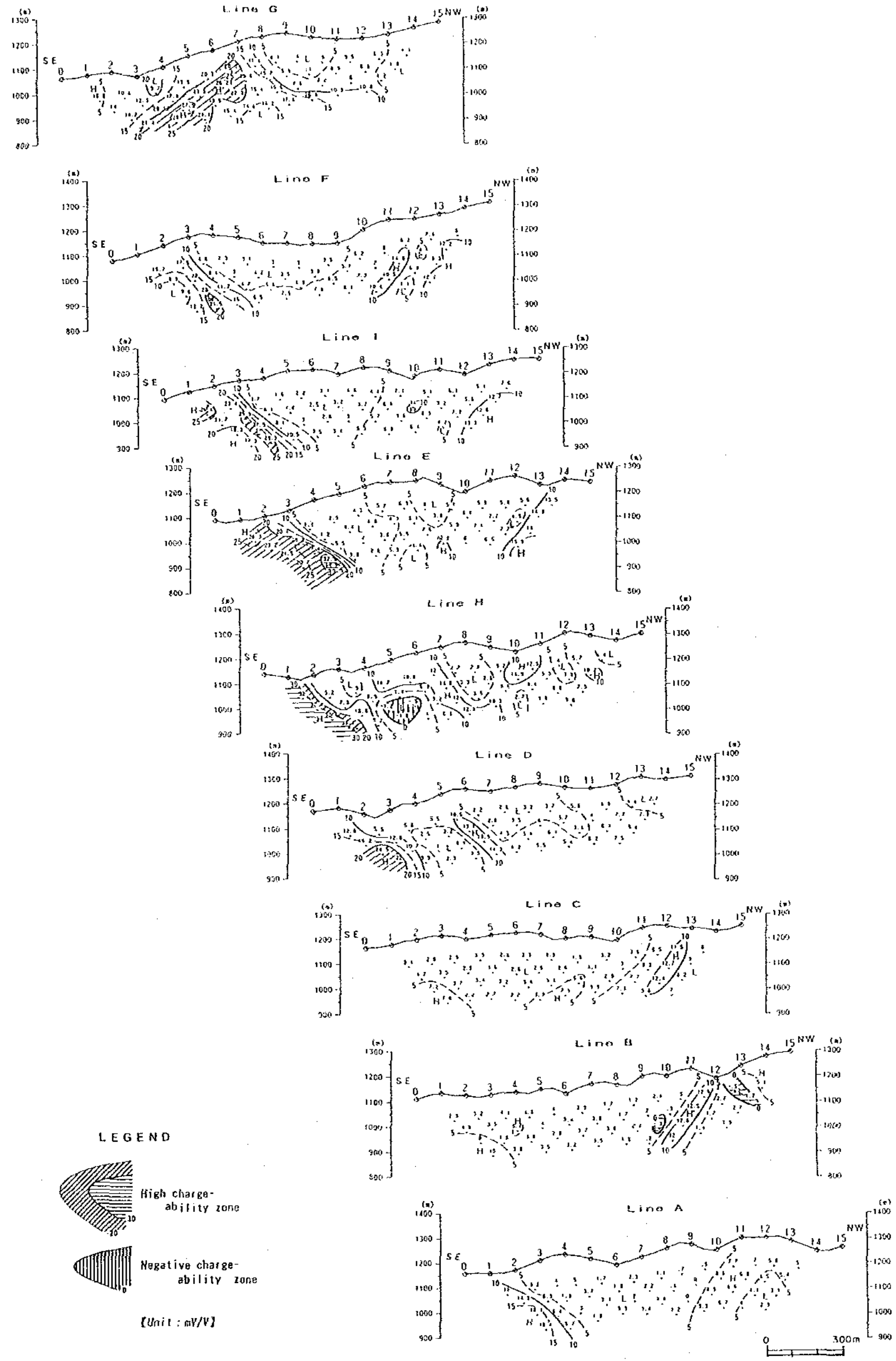

Fig. 3-7 Sections of Chargeability (Line A ～ I)

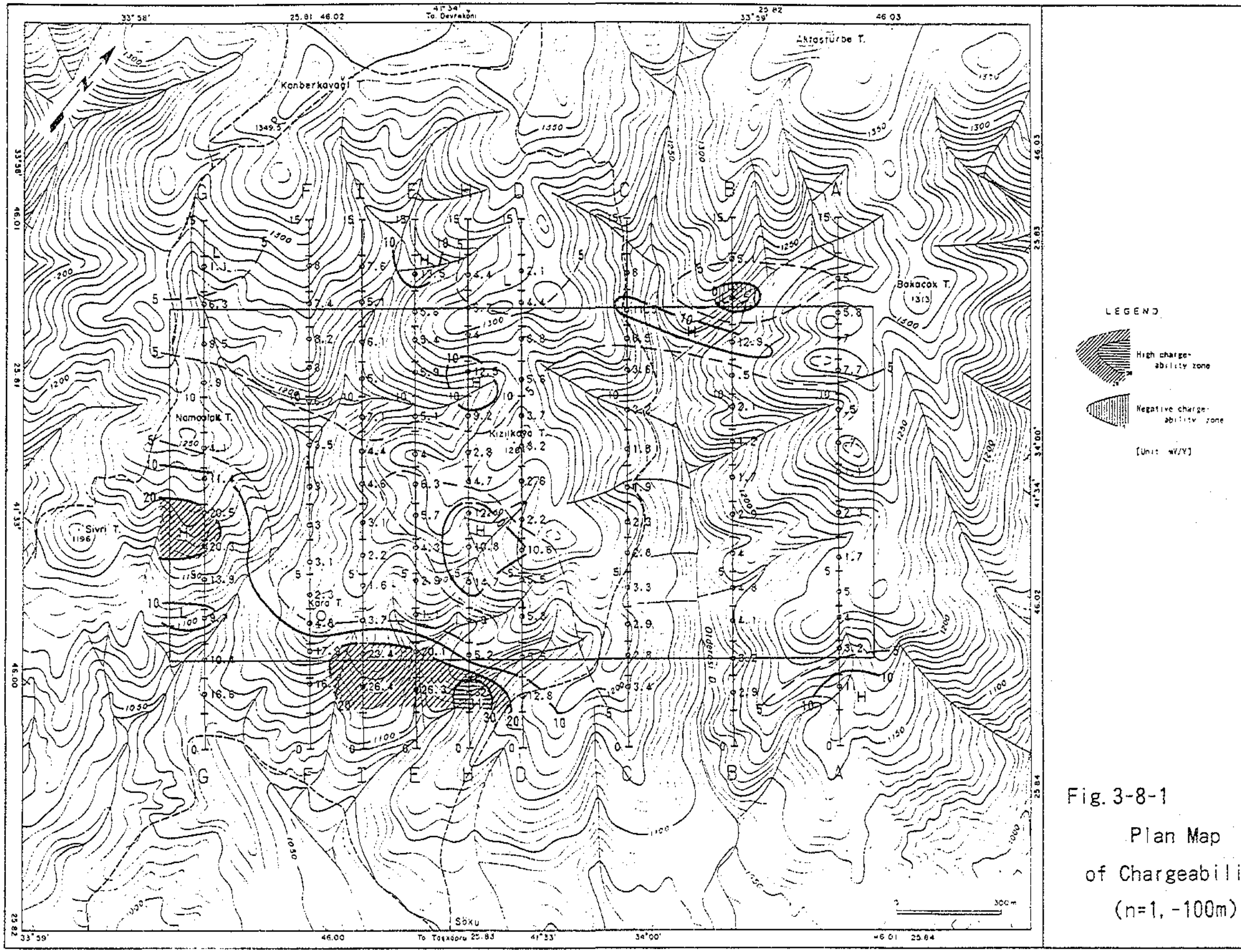

Fig. 3-8-1
Plan Map
of Chargeability
(n=1, -100m)

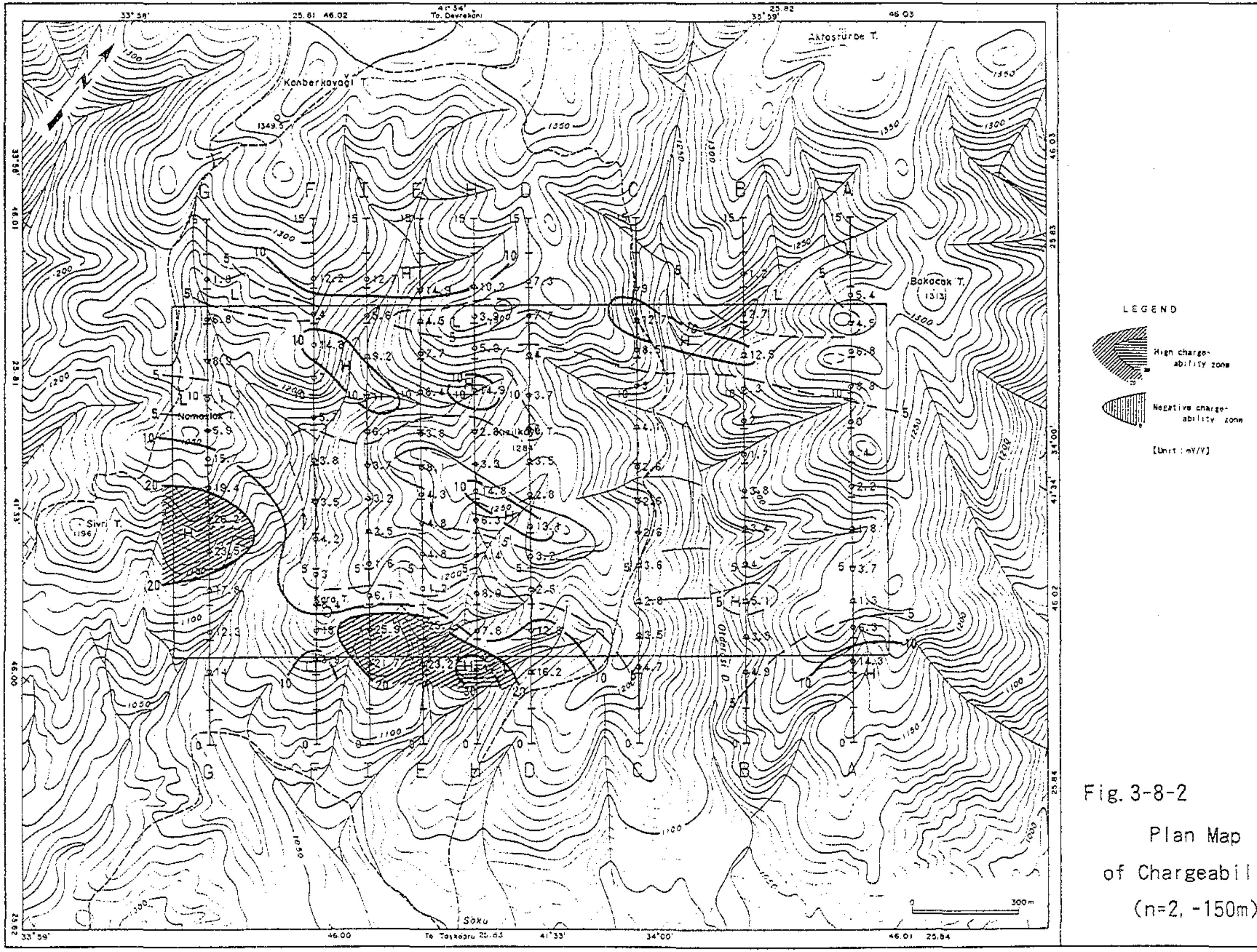

Fig. 3-8-2

Plan Map
of Chargeability
(n=2, -150m)

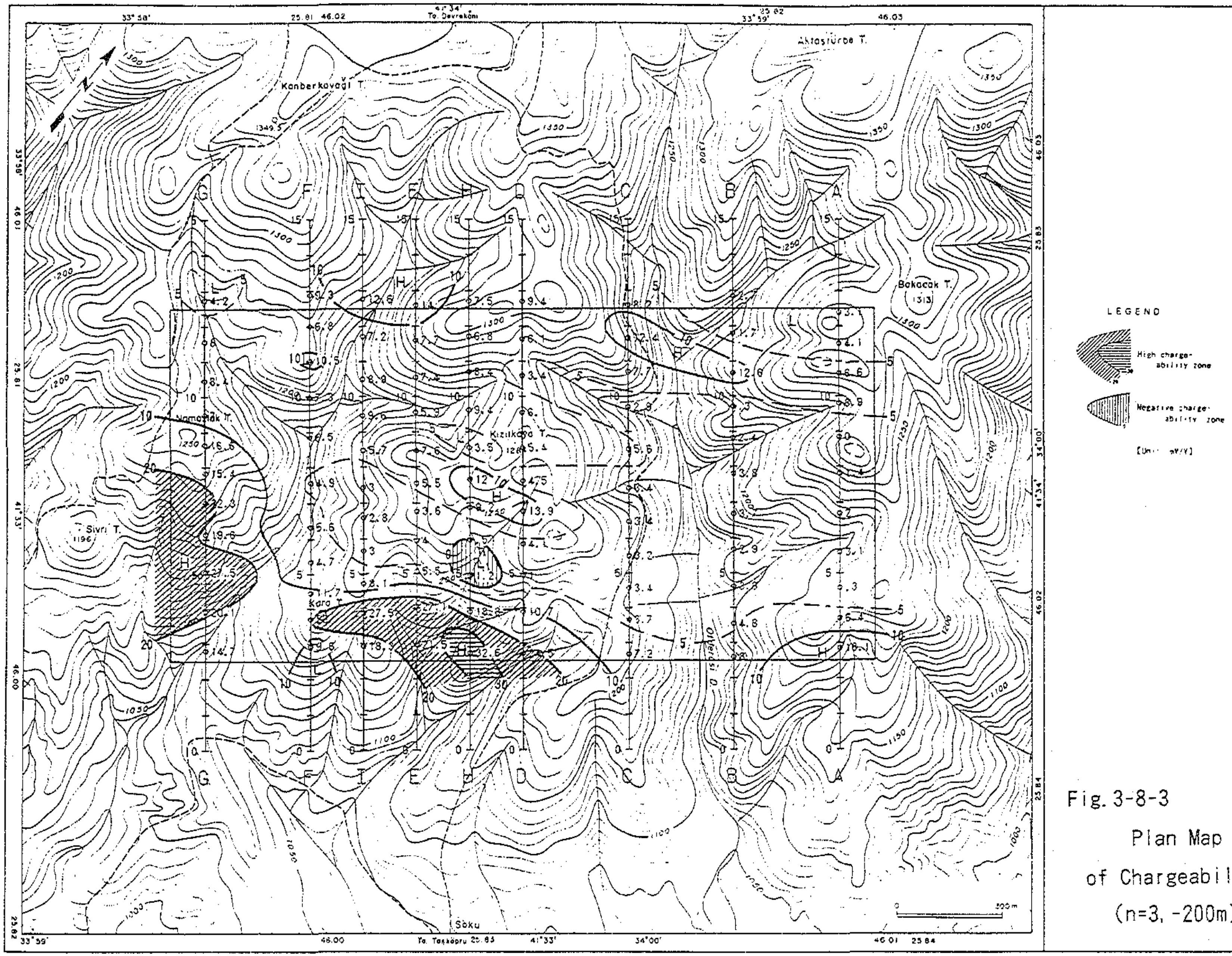

Fig. 3-8-3
Plan Map
of Chargeability
(n=3, -200m)

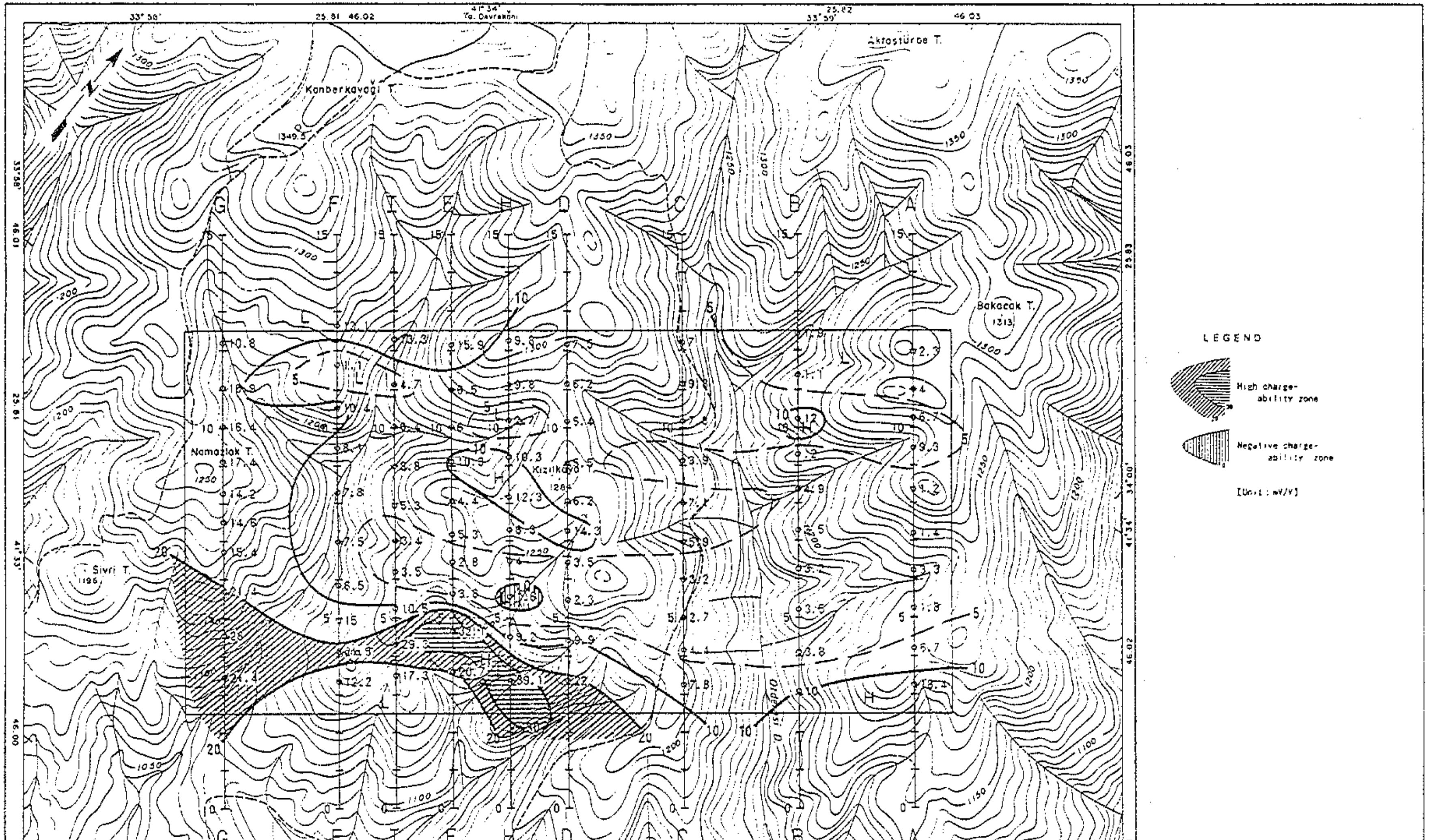

Fig. 3-8-4
Plan Map
of Chargeability
(n=4, -250m)

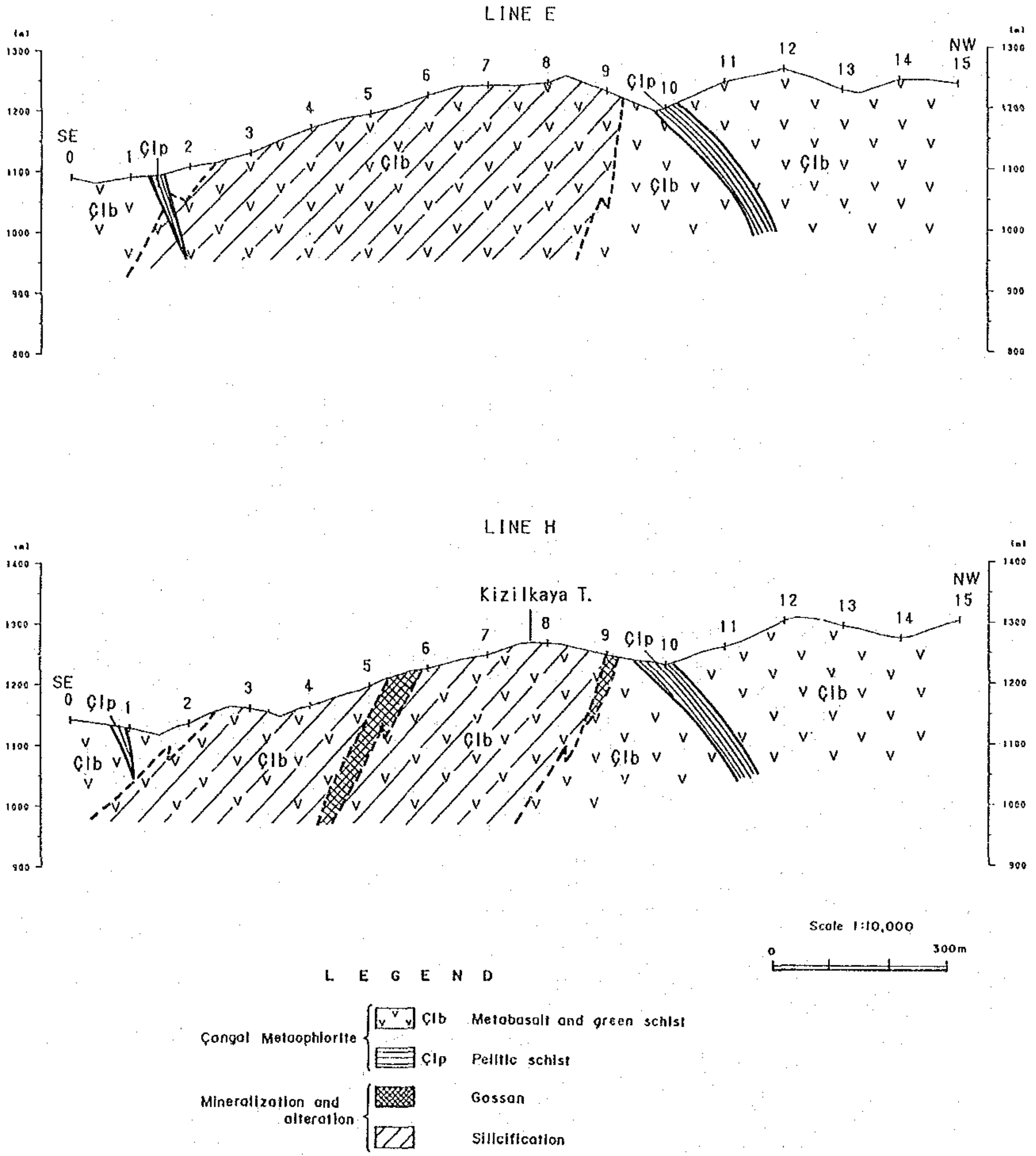

Fig. 3-9 Geological Sections of IP Survey Lines E & H in the Cünür Prospect

Simulation Model Line E

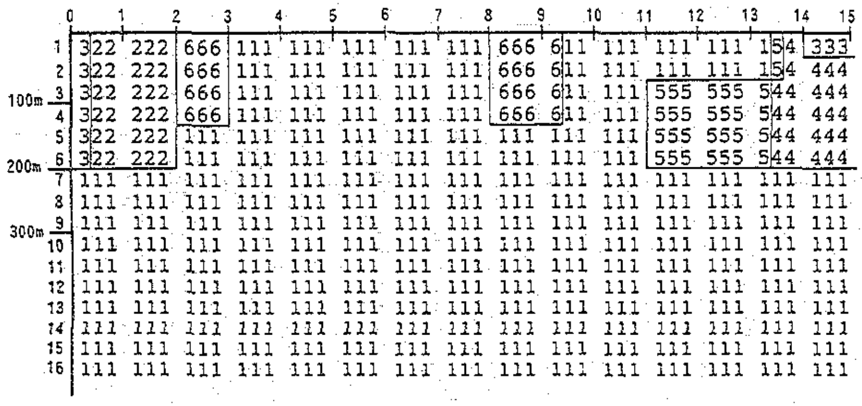

CODE	RESISTIVITY Ohm-m	CHARGEABILITY mV/V
1	150.	6.0
2	150.	30.0
3	150.	15.0
4	400.	15.0
5	400.	6.0
6	250.	6.0
7	0.	.0
8	0.	.0
9	0.	.0

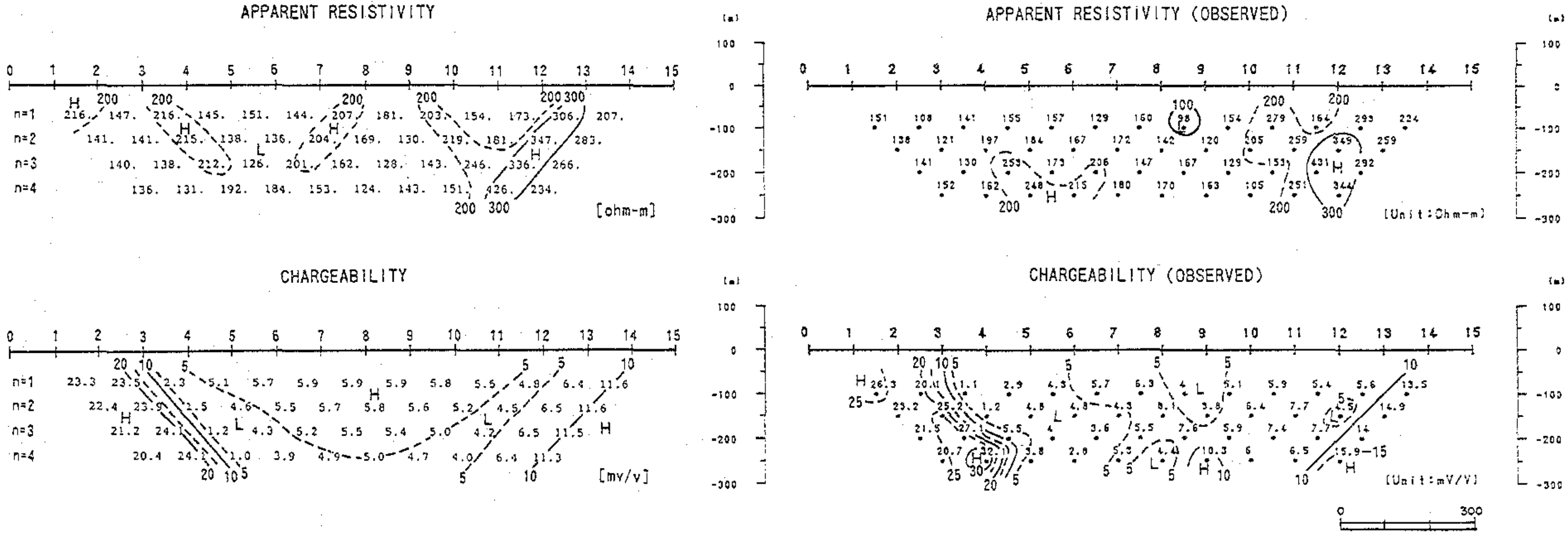

Fig. 3-10-1 Results of Two-dimensional Model Simulation (Line E)

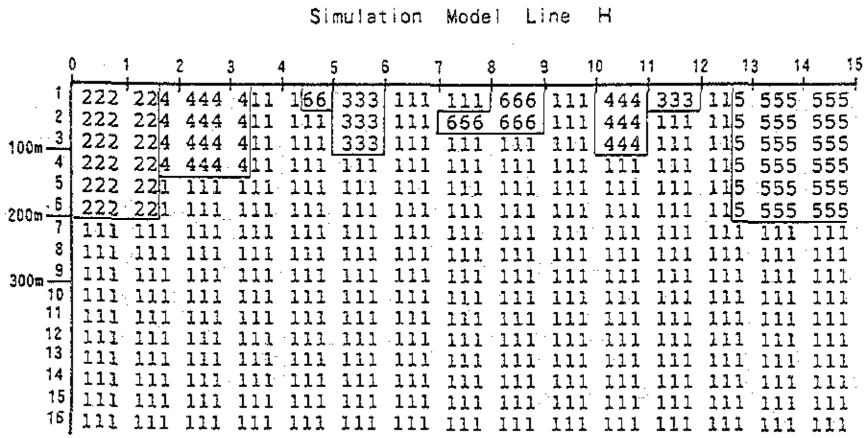

CODE	RESISTIVITY Ohm-m	CHARGEABILITY mV/V
1	150.	6.0
2	150.	40.0
3	150.	15.0
4	300.	6.0
5	600.	6.0
6	80.	6.0
7	0.	.0
8	0.	.0
9	0.	.0

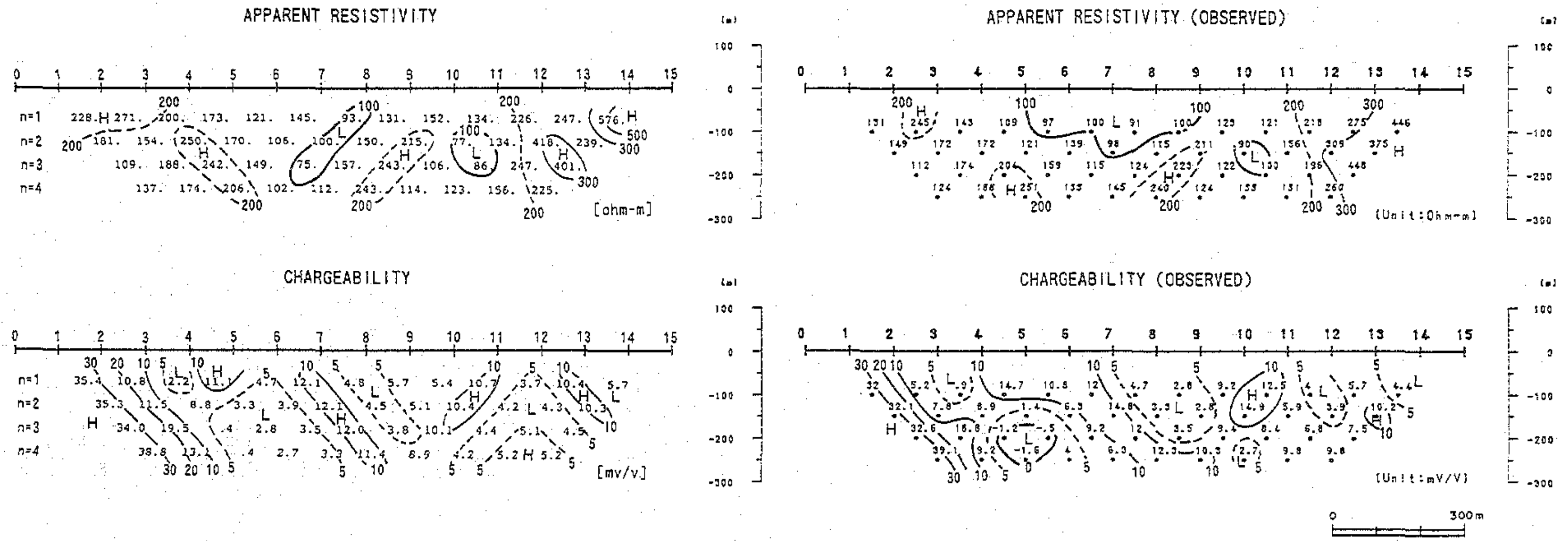

Fig. 3-10-2 Results of Two-dimensional Model Simulation (Line H)

No.9 of H, from which Cu 4.1% and Zn 1.4% were obtained in the previous year, the resistivity is within the background values and the chargeability is somewhat lower than the vicinity. Thus the mineralized zone is considered to be of small scale and probably has been oxidized and leached considerably because of the occurrence of azurite and chrysocolla. Extensive mineralization cannot be expected from this zone.

2-4 Results of Analysis - Cozoğlu Area

2-4-1 Measured Values

Apparent resistivity

The measured apparent resistivity values are shown for each line in Figure 3-12. The values are shown on plane maps for the four depths of -100m, -150m, -200m, -250m prepared by electrode separation index (Figs.3-13-1 to 3-13-4). The characteristics of these values are as follows.

a) Resistivity of 100ohm-m is dominant. The resistivity is generally higher to the north and lower in the central to southern parts.
b) High resistivity of over 300ohm-m is distributed in the northern side of the survey area and are detected in the shallow subsurface zones with the exception of Line C.
c) Low resistivity of under 30ohm-m is distributed in the E-W to WNW-ESE direction in the shallow zones of the central part of the survey area. These are detected in the sandstone and shale zones. Two small low zones are found in the deeper parts of Line A and one zone in Line G.

Chargeability

The measured values of chargeability are shown for each line on the profile (Fig.3-14). Also the values are determined by the coefficient of electrode separation for the four depths and are shown on plane maps (Figs.3-15-1 to 3-15-4). The following characteristics are noted.

a) Significant anomaly zones of over 50mV/V are detected in the central part of Lines A and B and also in the southern edge of the survey area.
b) The former anomalies are noted in the n=1 (-100m) and n=2 (-150m) plane maps, and they are weak anomalies of 30-50mV/V in the deeper parts. These anomalies coincide with the distribution of the slag near the Cozoğlu Village, but they extend eastward. The latter anomalies are detected at the profile ends throughout the Lines A - E and extend further southward.
c) Negative chargeability anomalies are detected in the central part of the survey area with WNW-ESE trend and also in the northeastern part with NE-SW trend. The former occurs widely corresponding to the sandstone and shale distribution, but is becomes narrower in the deeper parts. The latter anomalies are detected in the sandstone, shale and meta-basalt areas, but they become extinct at -200m and -250m depth.

Physical properties of rock samples

Resistivity and chargeability were measured by field equipment under field conditions in the laboratory for 11 samples collected from the surface in the field.

Table 3-2 Results of Rock Sample Measurement (Cozoğlu Prospect)

R o c k	No.	Chargeability	Resistivity	Remarks
Limestone	21	6.92(mV/V)	2,207	
Green schist	22	3.66	2,138	
Fine sandstone	23	4.78	1,740	
Coarse sandstone	24	6.29	890	
Siltstone	25	2.10	1,211	
Massive basalt	26	0.83	974	
Massive basalt	27	24.65	1,298	
Green schist	28	15.70	1,949	Pyrite dissemi.
Massive basalt	29	1.83	746	
Green schist	30	2.86	3,485	Few hematite
Slag	31	484.8	246	

The results are as follows.

a) Sample No. 31 is slag with high chargeability of 485 mV/V and low resistivity of 246ohm-m.
b) Other samples have chargeability of less than 10mV/V and high resistivity exceeding 750ohm-m with the exception of Nos. 27 and 28.

2-4-2 Results of Model Simulation Analysis

Model simulation was carried out for Lines A and B because significant chargeability anomalies were detected.

Line A:
Strong anomaly of 60mV/V was detected at the central part of the line and similar one in the southern edge of the Line.

The prepared model (Fig.3-17-1) has, at the central and southern end of the line, 50mV/V chargeability and 100ohm-m resistivity source by code 5 and low resistivity zone of 20ohm-m in the sandstone and shale zone.

The results of the simulation agree well with the measured values and thus this is considered to be a reasonable model.

The difference from the measured values is the lack of negative zone in the deep central part of the line, and the low value of the chargeability at the southern end.

Line B:

The characteristics of the chargeability and resistivity of this line is similar to those of Line A, and >50mV/V chargeability anomalies are detected in the central and southern parts of the line.

The prepared model (Fig.3-17-2) has a 100ohm-m, 50mV/V anomaly (code 5) in the central part of the line and this is smaller than that in Line A. The background is set at 100 ohm-m, 10 mV/V (code 1).

The result of the simulation is shown in the lower right of the figure and it is seen that they are harmonious with the measured results.

2-4-3 Discussions

Mineral showings were not observed on the surface by the first year geological survey in this area with the exception of slag. IP measurements were carried out during the present second year. Chargeability anomalies of 60mV/V were detected corresponding to the distribution of slag and also those of 30-50mV/V in the northwestern part and anomalies in the southern part in Lines A-E. The former anomalies extend further eastward and their western limit is inferred to be Line C. The resistivity is low at 50-100ohm-m, similar to that of sandstone and shale, and as this is not due to massive deposits, the possibility of the existence of large massive deposits is low. Of the latter anomalies, that of the southern end is confirmed by all lines, but the total feature is not clear because of the fact that it is at the end of the traverse lines. The anomaly is strong and it is continuous for significant distance. The shape of the anomaly suggests sulfide dissemination, but manifestations of mineralization are not found in the surface rocks (sandstone, shale, pelitic schist) of the anomalous zone.

Negative zones occur widely in the central and northwestern parts of the survey area and that of the central part corresponds almost completely with the sandstone and shale distribution. It is generally known in IP survey that negative anomalies occur from electromagnetic coupling, caused by electromagnetic coupling between the transmitting and receiving sides, or from artificial material such as power lines and pipelines. In the present area, however, there are only seven